Ministero dell'Istruzione, dell'Università e della Ricerca

Università degli studi di Palermo

Constraints on mantle source and interactions due to He-Ar isotope variations in Marsili seamount and eastern Aeolian Volcanic Arc (Panarea and Stromboli)

PhD thesis by:

Enrico Caruso

Tutor:

Prof. P.M. Nuccio

Co-tutors: **Dr. S. Bellia; Dr F. Italiano**

Coordinator of PhD Course:

Prof. F. Parello

DOTTORATO DI RICERCA IN GEOCHIMICA (GEO/08)

(XIX CICLO)

DIPARTIMENTO DI SCIENZE DELLA TERRA E DEL MARE (DISTEM)

Ministero dell'Istruzione,
dell'Università e della Ricerca

Università degli studi di Palermo

Constraints on mantle source and interactions due to He-Ar isotope variations in Marsili seamount and eastern Aeolian Volcanic Arc (Panarea and Stromboli)

PhD thesis by:
Enrico Caruso

Tutor:

Prof. P.M. Nuccio

Co-tutors:

Dr. S. Bellia; Dr F. Italiano

Coordinator of PhD Course:

Prof. F. Parello

Reviewers

R. Petrini
Dipartimento di Geoscienze
Università di Trieste

R. Trigila
Dipartimento di Scienze della Terra
Università di Roma

DOTTORATO DI RICERCA IN GEOCHIMICA (GEO/08)

(XIX CICLO)

DIPARTIMENTO DI SCIENZE DELLA TERRA E DEL MARE (DISTEM)

CONTENTS

1. INTRODUCTION

The southern Tyrrhenian Sea is the youngest volcanically active back-arc basin of the western Mediterranean, and is a complex geodynamic and geological system (Fig. 1.1). It is considered to be the result of subduction of the Ionian oceanic plate under the European plate (Barberi et al., 1974; Francalanci et al., 1993; Savelli, 2002).

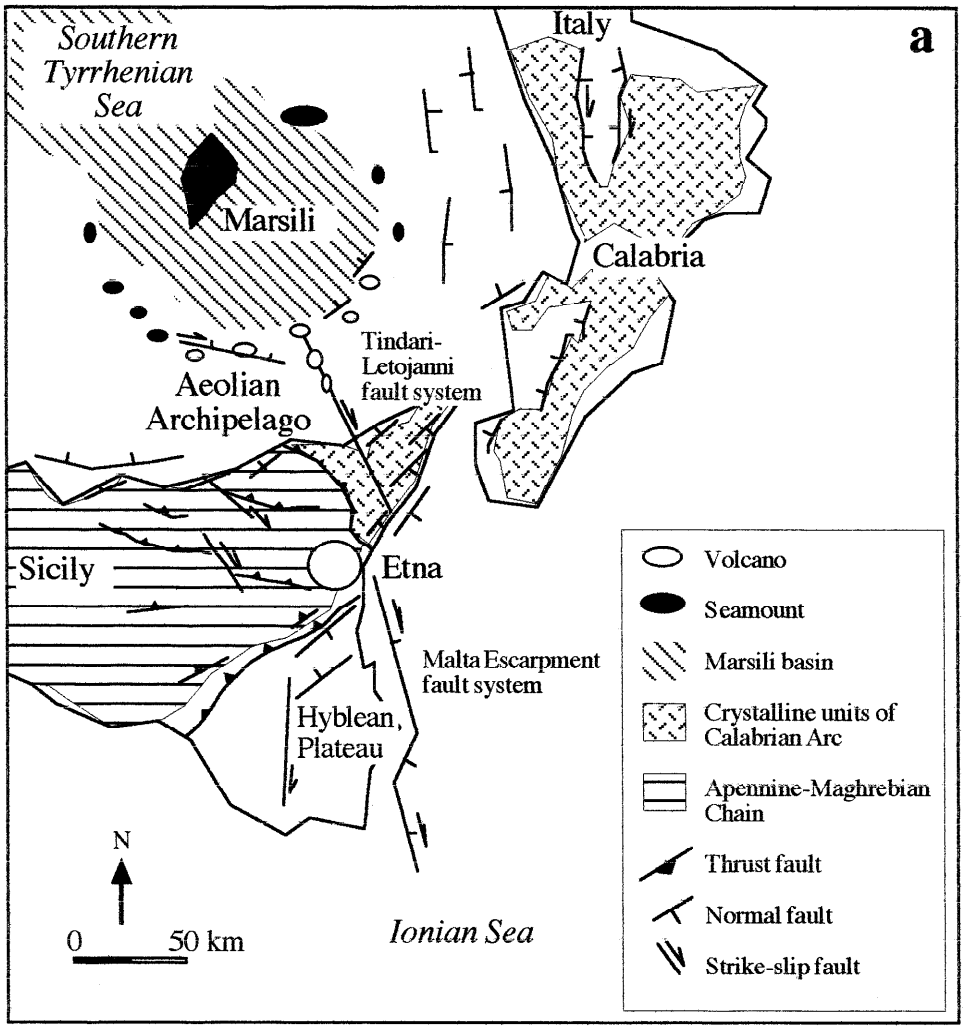

Figure 1.1 - *Geographical and structural sketch map of Southern Tyrrhenian Sea (From Ventura et al., 1999)*

The southern Tyrrhenian area developed from the Miocene to the Present within the framework of the coeval formation of the Apennine-Maghrebid Chain, structured above the north-western-subducting Ionian oceanic slab (Doglioni et al., 2004; Rosenbaum et al., 2004). Seismic studies reveal a thin crust about 15-20 km beneath the Aeolian arc (Piromallo and Morelli, 2003). It becomes thicker under the Calabrian peninsula (to about

25 km), but thins westward, reaching typical oceanic values of about 10 km in the Marsili basin.

The nature of the mantle under the Aeolian arc, in general, beneath Italy is still a matter of debate, and various sources have been proposed: a MORB-type mantle under the Aeolian arc (Francalanci et al., 1993); a HIMU-type mantle (that is, "high μ"; μ = $^{238}U/^{204}Pb$) mixed with shallow DM (Depleted Mantle) under the Tyrrhenian Sea (Gasperini et al., 2002); several upper-mantle domains beneath central-southern Italy (Peccerillo and Panza, 1999); and, lastly, a sub-continental mantle under the whole European continent (Dunai and Baur, 1995; Gautheron and Moreira, 2002).

Subduction processes involving oceanic (Ionian plate) and continental crust (final dipping stage of Adria micro-plate), aborted rifting (Pantelleria) and opening of back-arc basins (Tyrrhenian Sea) all make the Italian geodynamic setting varied and complex (fig. 1.2).

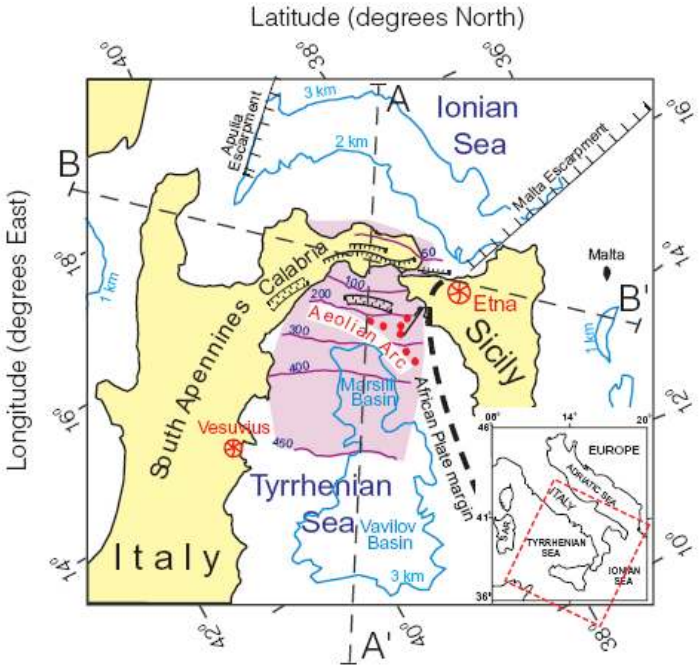

Figure 1.2 - *Map of the south Tyrrhenian subduction zone. The Ionian microplate subducts under the Tyrrhenian microplate (From Gvirtzman and Nur, 1999).*

Recent geological modeling (Gvirtzman and Nur, 1999) and geophysical studies (Chiarabba et al., 2008) suggest rapid south-eastward roll-back of the oceanic slab beneath the southern Tyrrhenian. Several authors (e.g., Trua et al., 2003; De Astis et al., 2006) hypothesize the lateral migration of African asthenospheric enriched mantle around the slab edges, into the colder mantle wedge. Ingress of the African mantle is demonstrated by the eruption of Ocean Island Basalt (OIB) magmas, anomalous in subduction-related

systems, at the northern slab edge environments (K- and Na-rich alkaline magma from the Vulture–Campania area), on the Italian mainland and southern ones (Na-alkaline magmas from the islands of Ustica and Prometeo) (Fig. 1.3).

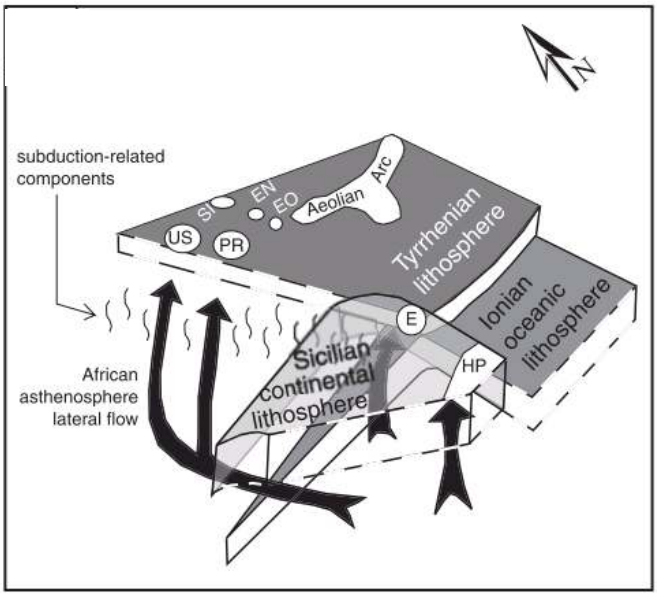

Figure 1.3 - *Subduction processes involving Ionian oceanic lithosphere and tyrrhenian lithosphere (From Trua et al., 2007)*

Quaternary IAB-type volcanic activity is represented by the Aeolian volcanic arc, the Marsili basin and the seamounts located in and around it. Petrologically, the related IAB-type volcanic rocks comprise calc-alkaline to shoshonitic products, with rare potassic rocks (Beccaluva et al., 1985; Tonarini et al., 2001b).

A major contribution to understanding of the nature and evolution of the Italian mantle has come from the study of trace elements, extensively carried out over the past twenty years. However, in order to discriminate between the various mantle sources and the possible contribution of the crust to arc magmas, helium takes on importance. Helium is a very powerful tracer, since the concentration of ^{3}He in oceanic and continental crust is practically zero (Poreda and Craig, 1989). In addition, as ^{4}He it is not produced in significant amounts by radioactive processes, it becomes an important factor revealing information on deep environments. The $^{3}He/^{4}He$ isotope ratio of oceanic arc basalts commonly fall in the range 6–8 Ra (where Ra is atmospheric $^{3}He/^{4}He$; 1.39×10^{-6}; Poreda and Craig, 1989). Values which are typical of normal mid-ocean ridge basalts (MORB) plot in the range 8 ± 1 Ra (Farley and Neroda, 1998). Helium in crustal fluids is enriched in radiogenic ^{4}He produced by the decay of U and Th. Crustal-radiogenic He is typically less than 0.1 Ra (O'Nions and Oxburgh, 1988). The absence of any significant contribution

of radiogenic He to oceanic arc basalts implies that subduction of altered oceanic crust and oceanic sediments does not enrich the mantle wedge in radiogenic helium. This is probable due to the loss of He from the subducting slab in the early stages of the process, before reaching the area of magma generation in the mantle wedge (Hilton et al., 1992, 2002).

In particular, fluid inclusions in phenocrysts generally preserve the He isotope ratio closest to the mantle source. In this hypothesis, which is the continuation and integration of research by Di Liberto (2003), new analyses of He isotope ratios from fluid inclusions trapped in olivine and pyroxene phenocrysts are presented for the islands of Panarea and Stromboli and the Marsili volcano. The isotope ratios of helium and argon in quartz xenoliths hosted by calc-alkaline lava of the Paleostromboli II period (Omo lavas) were measured and compared with those of Martelli et al. (2010) on the ultramafic lava xenoliths of San Bartolo lavas (Stromboli island).

2. GEOLOGICAL AND GEODYNAMIC SETTINGS

Southern Tyrrhenian Sea is a back-arc basin developed from Miocene to Present in the frame of the coeval formation of Apennine-Maghrebid Chain, structured above the north-western subducting Ionian oceanic slab (Doglioni et al., 2004; Rosenbaum et al., 2004). Its evolution has been characterized by great tectonic extension inducing volcanic activity and recent diffusing seismic activity, all migrated in space and time from North-West to South-East (Savelli, 1988; Beccaluva et al., 1994; Selvaggi and Chiarabba, 1995; Neri et al., 1996; Favali et al., 2004).

The geodynamic evolution of Sothern Tyrrhenian basin is morphologically evidenced by two main abyssal plains, the oceanic crust floored sub-basins of Vavilov (4.3–2.6 Ma) and Marsili (2 Ma), respectively; inside them the two greatest Tyrrhenian seamounts developed (Barberi et al., 1978; Kastens et al., 1990). In the surrounding areas of Marsili basin numerous other seamounts are located, representing the Western and North-Eastern submerged prosecution of the Aeolian Arc: Sisifo, Enarete, Eolo, Lametini, Alcione, Glabro and Palinuro.

The Moho depth is located 15-20 km below the Tyrrhenian abyssal plains and ~10 km beneath Vavilov and Marsili seamounts (Steinmetz et al., 1983; Locardi and Nicolich, 1988) corroborated with the following geophysical data. High resolution seismic reflection sections suggest a strong extensional setting of the Tyrrhenian basin (Finetti, 2004).

An extremely high heat flow with regional values around 120 mW/m^2 and local maxima in correspondence of Vavilov (140 mW/m^2) and Marsili (250 mW/m^2) areas has been recorded (Della Vedova et al., 2001; Mongelli et al., 2004). Furthermore, on the uppermost and central portions of Vavilov and Marsili volcanoes, heat flow achieves 300 and 500 mW/m2, respectively (Verzhbitskii, 2007). These positive heat flow anomalies coincide with gravity and magnetic ones (Faggioni et al., 1995; Cella et al., 1998). Thus, the geophysical data strongly suggest the presence of magmatic bodies intruding shallow, thinned and stretched crustal levels. In turn, the diffuse and localised high heat flows are related to the upraising of basaltic melts at lower depth below the Tyrrhenian sea-floor. Therefore, volcanic Tyrrhenian seamounts can be considered huge heat sources; and the Marsili seamount is the most intense one.

2.1 Marsili seamount

The Marsili seamount rises 3500 m from the abyssal plain to 489 m minimum depth. The volcanic edifice is about 60 km long and about 20 km wide (Fig.2.1). The dimensions and the distinctive morphology of the Marsili volcano are suggested to result from the superinflation of a spreading ridge, attributed to a higher than normal magma production (Marani and Trua, 2002).

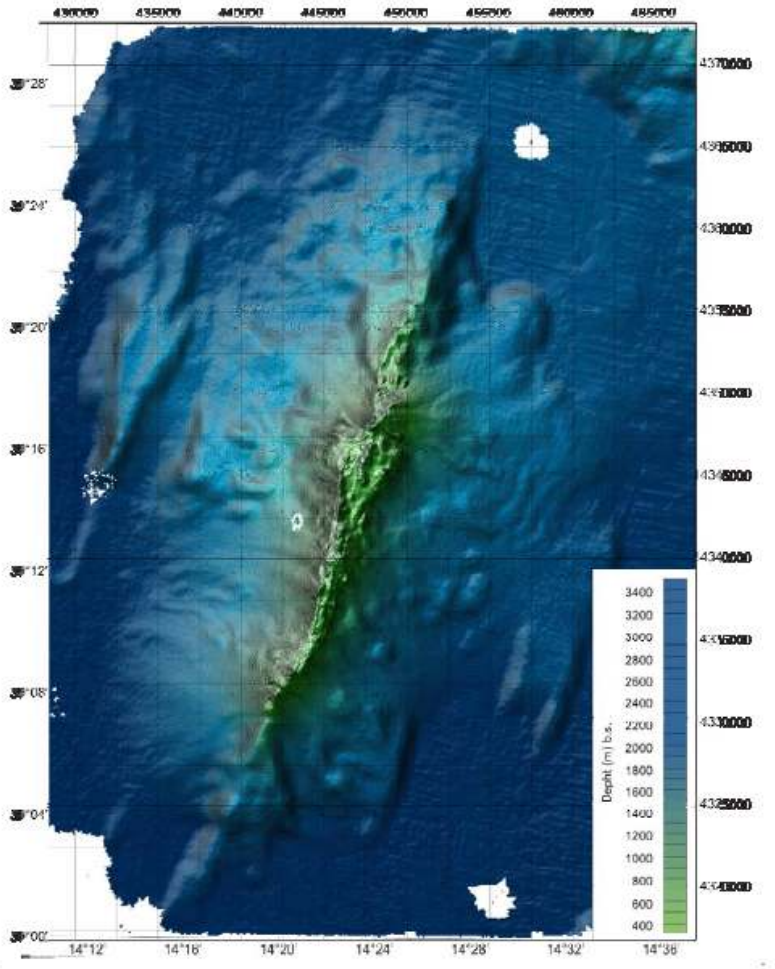

Figure 2.1 – *Bathimetric and morphologic map of Marsili volcano (From Caso et al., 2010)*

As the spreading rate of the Marsili back arc basin did not significantly change during the growth of the Marsili volcano, which began construction 0.7 Ma ago, it has been suggested that the excess magma production of the volcano was related to melting of the underlying mantle wedge. Melting was triggered by the lateral ingression of hot asthenospheric fluxes of African mantle around the edges, and ultimately over the top of the Ionian slab, which lies 350 km depth beneath the Marsili volcano.

The southern Tyrrhenian sea, back-arc basin magmatic activity is characterised by eruption of a wide range of magmas that requires the involvement of at least four distinct mantle source: IAB, MORB, and OIB-type, and a mantle source generated by subduction related enrichment of the OIB-type mantle source (Trua et al., 2004a; Trua et al., 2004b). Magma derived from an IAB-type mantle are by far the most common and cover most of the known subduction related volcanic suites of the southern Tyrrhenian basin. These magmas includes: calc-alkaline and shoshonites rocks of the Marsili and Vavilov basins, the Marsili seamount, the Anchise seamount and the Aeolian islands and related seamounts; arc tholeiites recovered from Lamentini seamount; and potassic rocks present at Vulcano and Stromboli island, and probably also present in the Albatros seamount. Magmas derived from a MORB-type mantle were only recovered from the Vavilov back-arc basin. Magmas derived from an OIB-type mantle coexist with magmas derived from the IAB-type mantle source in both Vavilov and Marsili backarc basins, although the former are restricted to a few areas: the Magnaghi, Vavilov and Aceste seamounts. Finally, the potassic and ultrapotassic magmas of the eastern margin of the southern Tyrrhenian sea can be related to an OIB-type mantle source enriched by subduction-related components.

2.2 Aeolian Arc

The Aeolian arc is an archipelago of seven volcanic islands and several seamounts, located close to the north-eastern Sicilian coast (fig. 2.2), and represents an expression of the Italian quaternary magmatism that took place in a subduction related setting.

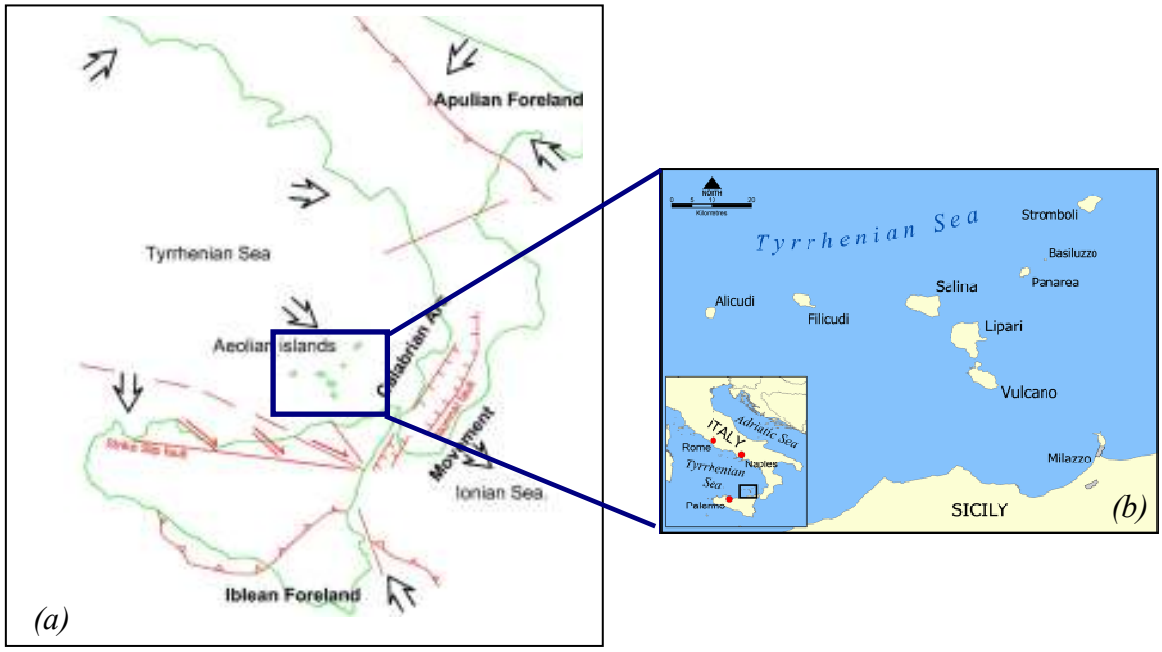

Figure 2.2- *(a) Simplified sketch of the tectonic setting (red lines) of Southern Italy.(b) Geographical map of Aeolian islands*

Volcanic activity presently occurs at Stromboli, Vulcano and Panarea, with lavas and pyroclastic products in the first island and fumarolic activity in the others; volcanic activity occurred at Lipari in historical time (Pichler, 1980).

The volcanism of this area evolved over a short period of time (1 Myr). Its magmatological features change from the calc-alkaline (CA) series of Alicudi and Filicudi to the high potassium (HKCA) and shoshonitic (SHO) series of the present activity shown by Vulcano and Stromboli (Barberi et al., 1974; Ellam and Harmon, 1990; Francalanci et al., 1993; De Astis et al., 2000). Tholeiitic rocks have also been dredged up from the sea floor of the area (Beccaluva et al., 1982).

The transition from CA to HKCA and SHO magmas is one of the most significant issues of the Aeolian magmatism and has significant implications as far as the genesis and evolution magma models and mantle source characterization are concerned.

Recent studies (Calanchi et al., 2002) have highlighted many differences between the western and the eastern sector of the arc in terms of the increase in both the $^{87}Sr/^{86}Sr$ isotope ratio and HFSE concentration and the decrease in the LILE/HFSE ratios. Moreover, strong resemblances between the isotope features and the incompatible element ratios of the Stromboli and mafic rocks from active Campanian volcanoes (Vesuvio and Phlegrean Fields) have been noticed. Accordingly, Gasperini et al. (2002) considered the Campanian and Aeolian magmas as being a transition term from the Latium-Tuscany magmatism to that of Mount Etna.

Most authors have described the variations in many incompatible elements and in the Sr, Nd and Pb isotope ratios in the Aeolian arc in terms of the possible mixing of a mantle source with a crustal component (Ellam et al., 1988; Francalanci, Taylor et al., 1993; Calanchi et al., 2002; Gasperini et al., 2002).

The Aeolian archipelago was previously considered as being a single structure related to the subduction zone (Gasparini et al., 1982; Ellam et al., 1989); nevertheless recent geophysical and geochemical data and a structural analysis of the arc suggest that it could be separated into two different sectors: a western one and an eastern one, divided by the islands of Vulcano and Lipari (Calanchi et al., 2002). Regional fault systems oriented E-W, NW-SE and NE-SW strongly control the distribution of volcanoes (Calanchi et al., 2002). In particular, the islands of the western sector were built up along an en-echelon dextral strike-slip fault system with a predominant WNW-ESE direction (Finetti and Del Ben, 1986). In the central part of the arc, Salina lies on the intersection between the western

sector and the Lipari-Vulcano alignment, the northern extension of the Tindari-Letoianni-Malta escarpment transcurrent fault (Gasperini et al., 2002).

In the eastern sector of the arc, the NE-SW-trending extensional structures control the islands of Panarea and Stromboli (Beccaluva et al., 1985; Gabbianelli et al., 1993).

The islands of Alicudi and Filicudi represent the typical mafic and intermediate CA terms with relatively un-radiogenic strontium isotopes. On the easternmost side, Stromboli displays a full evolution of the magmatic terms (CA - HKCA - SHO), showing the highest radiogenic strontium signature with a strong affinity to the Campanian magmatism. This affinity led some researchers to hypothesise a similar mantle source (Peccerillo and Panza, 1999; De Astis et al., 2000; Peccerillo, 2001).

A seismic zone beneath the Aeolian arc dips 50°- 60° in an approximately NW direction under the Tyrrhenian Sea (Barberi et al., 1973). The location of the Aeolian arc is on the continental slope that separates Sicily from the Tyrrhenian abyssal plane at the boundary between the African and the European plates (fig.2.2). The continental nature on both sides of the plate boundary (Finetti and Morelli, 1972) and the occurrence of shoshonitic rocks suggests that the Aeolian arc is in a senile stage of its evolution. Starting from this point, some authors (Francalanci, Taylor et al., 1993) pointed out that the lower continental crust could also possibly have been involved in the subduction process under the eastern sector of the Aeolian arc; nevertheless the geochemical characteristics of the vulcanite's erupted in Central Campania and in the Aeolian Islands suggest that the nature of the slab beneath the Calabrian arc is oceanic (Beccaluva et al., 1989; Serri et al., 1990).

The subduction of the Ionian plate most probably is at the origin of the Aeolian arc formation and represents the last stage of the Apennine collision.

This process started 30 Myr ago with the westward subduction of the Adria plate under the European margin, (Doglioni et al., 1999) and ended about 13 Myr ago with the collision between the continental crusts of the two plates (Beccaluva et al., 1985). As a result of this collision, the subduction rotated the direction of convergence to the northwest with the opening of the Tyrrenian Sea as a back arc basin about 8 Myr ago (Beccaluva et al., 1990). The absence of deep earthquakes in central Italy indicates that there is no active shallow subduction in this area (Westaway, 1992). On the contrary, the subduction of the oceanic Ionian plate is currently active beneath Sicily coherently with the sismicity, at depths of 200-500 Km, ubiquitous under the southeastern Tyrrhenian Sea (Istituto Nazionale di Geofisica, unpublished data, from Gasperini et al., 2002) (Fig.2.3).

The northern and the southern parts of the subducting plate have different directions and subduction velocities, about 1 cm/yr for the passive subduction (i.e. gravitational sinking) under Tuscany and 5 cm/yr for the active subduction under Sicily, and this is the cause of a differential in the subduction length between the two ends of the plate, in part absorbed by trench roll-back and the counter clockwise rotation of Italy (Gasperini et al., 2002).

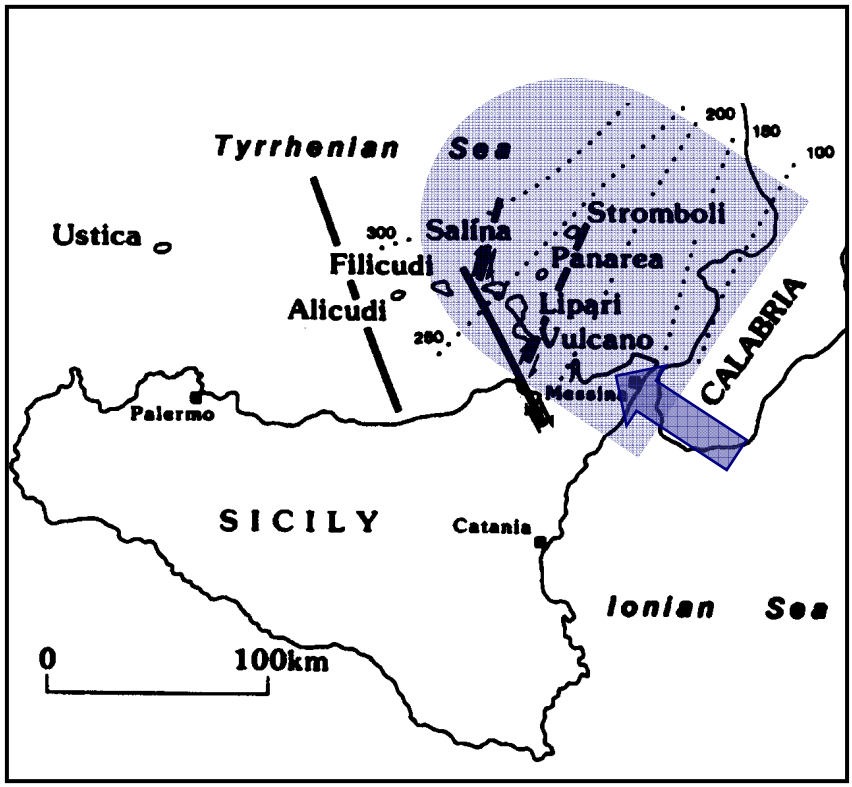

Figure 2.3- *Depth to the Benioff zone under the Aeolian arc (after Ellam et al., 1988, modified); Dashed contours show the depth to the Benioff zone in Km, the solid lines indicate strike-slip faults.*

Coherently with the high-resolution tomographic model of Piromallo and Morelli (1997), where a 400 km-wide gap is observed under Vesuvius at a depth of 150 km in the high-velocity material (representing the subducting plate), Gasperini et al. (2002) envisage the rupture of the plate corresponding to a broad window in the Adria plate under southern Italy. On the contrary, De Gori et al. (2001) propose a tomographic model where an almost continuous slab is indicated under the Apennines; Gvirtzman and Nur (2001) indicate a complete break-off of the subducted lithosphere under the Apennine zone and a strong pull-down related to a rapid rollback of the oceanic slab under the South Tyrrhenian Sea without the rupture of the dipping plate (Fig. 2.4).

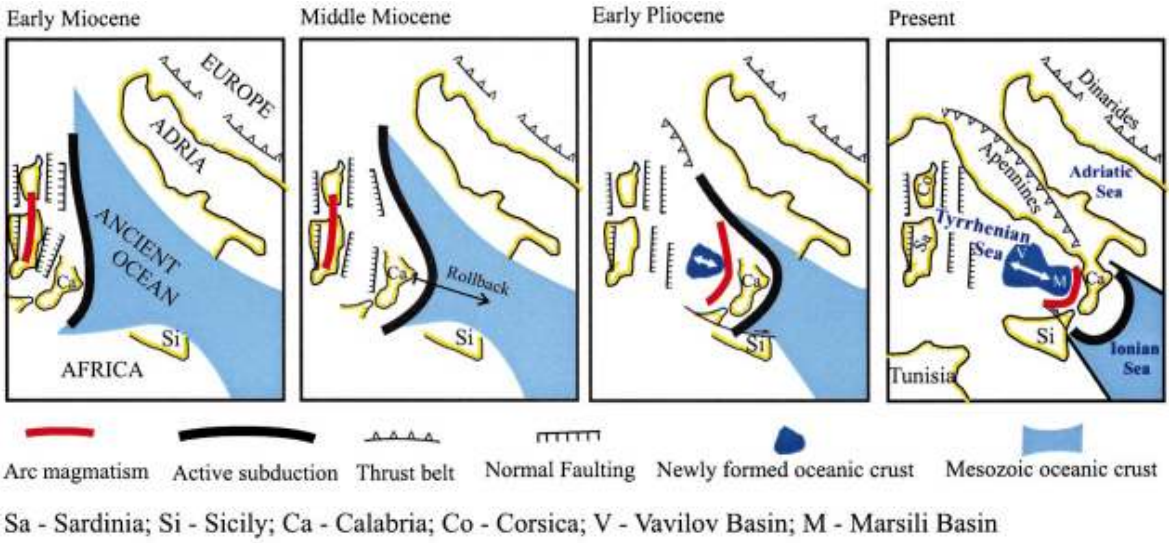

Figure 2.4 - *Schematic palinspastic reconstruction of the central Mediterranean since Miocene (from Gvirtzman and Nur, 2001)*

3. LOCATION AND BRIEF DESCRIPTION OF SAMPLES

To determine the He and Ar isotope composition of the mantle beneath southern Tyrrhenian sea, fluid-inclusion study has been performed on quartzite nodules of Stromboli volcano hosted by calcalkaline lavas and fresh olivine and/or pyroxene were sampled from Panarea, Stromboli and Marsili volcano. Details of sample location and rock-type are given in Table I (Appendix A).

To following a brief petrographic description of rock samples taken at Stromboli, Panarea and Marsili volcano.

3.3 Marsili volcano

The submarine volcanic samples analysed in this study have been recovered during oceanographic cruises (Marani et al., 1999; Trua et al., 2003, 2004a, 2004b), and have been furnished by Dr. Italiano, INGV sez. Palermo. The sampled rocks are aphyric or with a low porphiricity index. Only MRS 04 porphiric sample was selected in order to analyze noble gases in fluid inclusions. MRS 04 is characterized by a basaltic composition (see fig. 3.5 TAS diagram). Chemical analyses are reported in tab II (Appendix B).

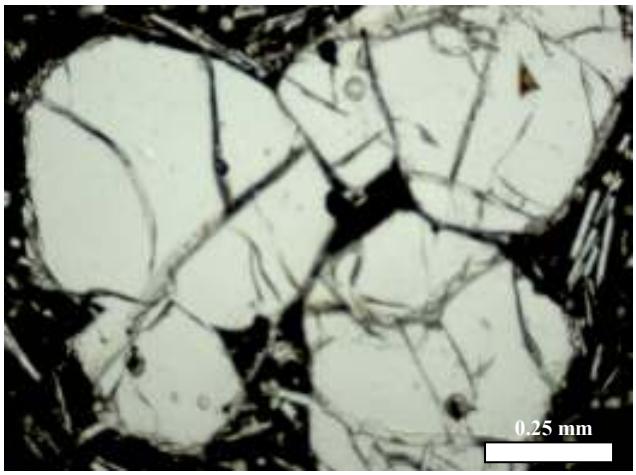

Figure 3.5 *- Olivine morphology is euhedral, in the range of 1-2 mm in diameter, and it occasionally contains Cr-spinel inclusions.*

The MRS 04 lava is characterized by vesicular textures. Vesicles vary from irregular to sub-spherical shape, in the range of 1-6 mm in diameter. MRS 04 natural mineral assemblage includes plagioclase and olivine as the dominant phases, and cpx in minor abundance. Olivine morphology is euhedral, in the range of 1-2 mm in diameter; crystals occasionally contain Cr-spinel inclusions. Olivine SEM-EDS analyses reveal high forsteritic components (Fo_{89-90}) with a Fe-Mg exchange coefficient ($Kd^{Fe\text{-}Mg}{}_{ol\text{-}liq}$) = 0.24 (calculated considering the liquid as whole rock), approaching to the equilibrium value (Kd = 0.26) Di Carlo et al., 2006.

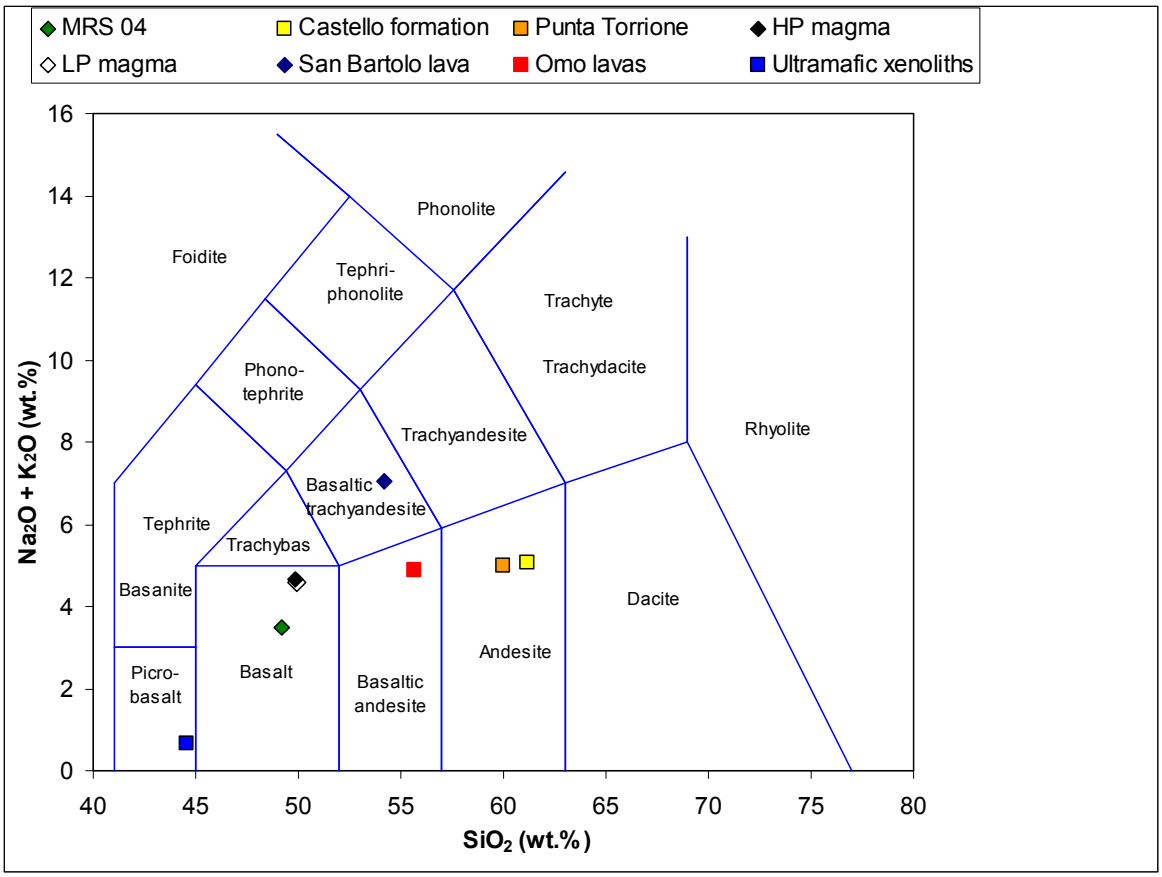

Figure 3.5 *– Total Alkali vs. silica classification diagram (Le Bas et al.,1986) for Neogene-Quaternary southern Tyrrhenian volcanic rocks. Ultramafic xenoliths data from (Laiolo and Cigolini, 2006).*

3.1 Stromboli island

HP and LP magma

Two types of magma, mainly differing in crystal and volatile contents, have fed the volcano since the beginning of its persistent activity: a highly porphyritic magma (HP-magma), erupted as scoriaceous bombs, lapilli and lavas during the normal activity and effusive episodes, and a volatile-rich, aphyric to slightly porphyritic magma, with low phenocryst contents (LP-magma), which is emitted as pumices only during paroxysms. The latter is usually mingled with the HP-magma (Fig. 3.1), mainly due to syn-eruptive processes (Bonaccorso et al., 1996; Bertagnini et al., 1999; Francalanci et al., 1999; Rosi et al., 2000). The HP-magmas are high-K shoshonitic basalts with a phenocryst content of ~50 vol.% and a volatile content 0.60 wt.%. The LP-magmas are slightly less evolved high-K basalts, with lower silica and K_2O contents than the HP-magmas (SiO_2 48.2–49.2 wt.% and 48.6–51.5 wt.%, and K_2O1.5–2 wt.% and 2–2.5 wt.%, respectively. They show a crystal content <5% vol, with high volatile contents up to 3.4 wt.% (Métrich et al., 2001; Bertagnini et al., 2003). The HP-magmas have slightly higher incompatible trace element contents, except for Sr, and lower MgO and compatible trace element abundances than LP-magmas (Francalanci et al., 2004).

Volatile-rich magmas are thought to originate in the lower part of the plumbing system, whereas HP-magmas are associated with a shallow reservoir and result from the crystallisation of the LP-magma, mainly driven by decompression and water loss at low pressure, associated with minor crystal fractionation and recycling of old crystals. The latter are brought into the shallow reservoir by the replenishing LP magma (Francalanci, 1993; Francalanci et al., 1999, 2004, 2005; Métrich et al., 2001; Bertagnini et al., 2003; Vagelli et al., 2003; Landi et al., 2004). Accordingly, the dynamics of the shallow magmatic system has been envisioned as a steady state, continuously erupting and crystallising magma chamber that is replenished at a constant rate by the LP-magma.

Mixing and olivine+clinopyroxene+plagioclase crystallisation control the evolution of the magmas feeding the present-day activity of Stromboli (Armienti et al., 2007).

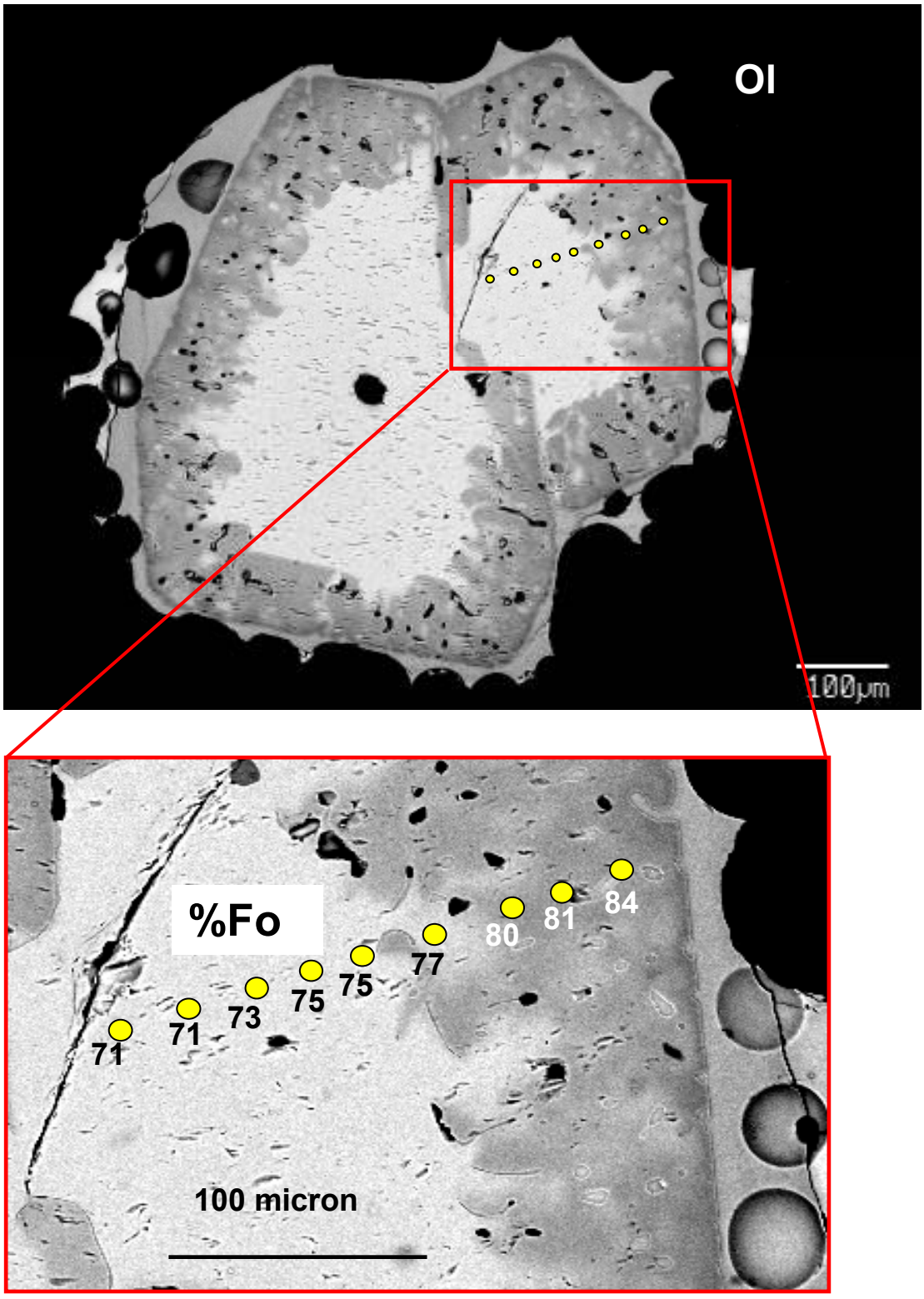

Figure 3.1 *- LP pumice: selected olivine between 0.5 e 1 mm, rich in bubbles. Chemical composition: between Fo71 and Fo90, mingling with HP within a single crystal, da Martelli et al.,2010*

Quartz xenoliths

The samples studied are represented by quartz xenoliths hosted by calc-alkaline basaltic andesite lavas of both the Paleostromboli II period (about 60 ka). The size of the xenoliths varies from a few to about 10 cm. They are mainly made up of quartz grains of different shapes and sizes (Vaggelli et al, 2003). The outer contact with host lavas is commonly sharp and characterised by the presence of a coronitic texture mainly constituted by prismatic clinopyroxene microcrystals, elongated perpendicular to the contact interface and, subordinately, by interstitial plagioclase, K- feldspar and glass.

These quartzites are restites from partial melting, involving felsic crustal rocks at the magma/wall rock contact. Restitic quartz re-crystallises at variable and generally high temperatures, leading to the formation of quartzites with different textures (Fig 3.2).

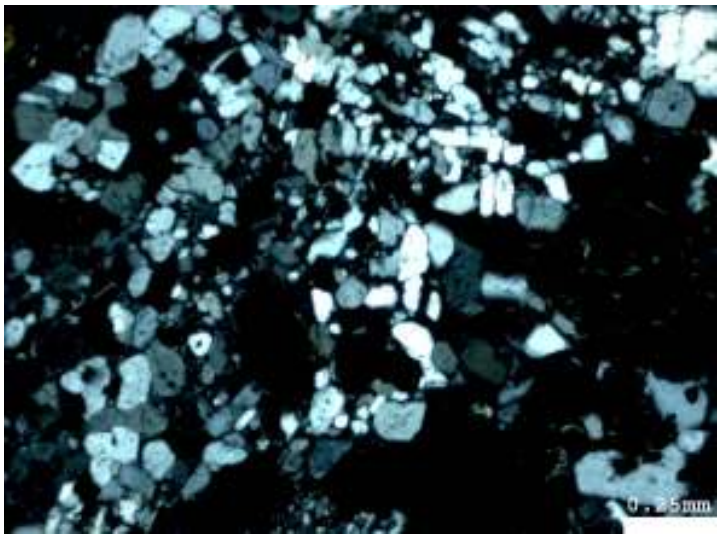

Figure 3.2 *- Inequigranular granoblastic nodules with medium/large re-crystallised quartz crystals.*

Ultramafic xenoliths

Ultramafic xenoliths are represented within a large basaltic lava field of Stromboli, known as San Bartolo lavas (high-K calc-alkaline –HKCA, erupted <5 ka BP) and consist of dunite and wehrlite. Thermobarometric studies estimated for the crystallization of gabbroic materials a minima equilibration pressures of 0.17–0.24 GPa, at temperatures ranging from 940 to 1030◦C (Cigolini et al., 2006). These materials interacted with hydrous ascending HKCA basaltic magmas (with temperatures of 1050–1100°C) at pressures of about 0.2–0.4 GPa. These pressure regimes are nearly identical to those found for the crystallization of phenocrystic phases within HKCA basaltic lavas. Dunite and wehrlite show

porphyroclastic-heterogranular textures. These ultramafic materials are in equilibrium with more primitive basaltic magmas (under moderately hydrous and anhydrous conditions) at pressures of 0.8–1.2 GPa, which is below the crust-mantle transition, located at about 20 km depth under Stromboli (Laiolo and Cigolini, 2006).

3.2 Panarea island

A Panarea were collected several representative samples of different rock types. Only two samples (Castello formation and Punta Torrione) it was possible to carry out the analysis of noble gases. The other samples show a low gas content in fluid inclusions., it cannot to measure the gas noble contents and isotope ratios.

Castello formation

The sample Castello formation consists of high-K calc-alkaline andesite. This sample exhibits intersertal or porphyritic seriate textures with phenocrysts of plagioclase, clinopyroxene, orthopyroxene, and rare amphibole; the latter is completely transformed to opaque oxides (Fig. 3.3). The porphyritic index (P.I.) is in the range 30-20%. Plagioclase makes up more than 50% of the phenocryst content and consists of complexly zoned and twinned crystals with anorthite contents between An_{80} and An_{35}. Clinopyroxene phenocrysts show very limited compositional variability; orthopyroxene show both normal and reverse zoning .

Punta Torrione

Thick bedded, massive, brown tuff, locally rich millimetric euhedral Cpx crystals (Fig. 3.4). Formed by millimetric glass fragments, it exhibits CA basaltic andesite composition. Lucchi et al. (2010) have recently suggested that the source of brown tuff is located beyond Panarea, within the La Fossa Caldera of Vulcano.

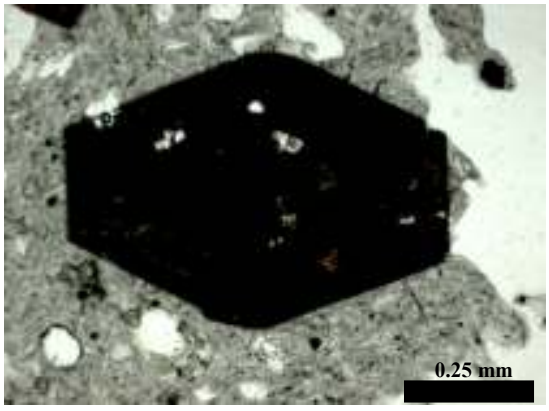

Figure 3.3 - *Amphibole is completely transformed to opaque oxides*

Figure 3.4 - *Millimetric euhedral Cpx crystals from brown tuff.*

4. EXPERIMENTAL TECHNIQUES

Rock samples were crushed to a grain size below 2 mm, taking into account that most of the minerals have a grain size below 1 mm. Then 0.5 mm crystals were selected by hand under a binocular microscope. Separated minerals were ultrasonically cleaned in 5% HNO_3, and then in distilled water and high-purity acetone. During each analytical session, about 1 g of olivines or 2 g of pyroxenes were loaded in the crusher and pumped to an ultra high vacuum overnight baking at 130 °C. The loaded quantities above reported were established considering the expected amount of noble gases produced by crushing. Gases were extracted by in-vacuo crushing at about 200 bar pressure, so as to minimize the contribution of noble gases in the crystal lattice due to radioactive decay (Hilton et al., 1999). Helium, neon, and argon were cleaned up in a stainless steel ultra- high-vacuum line, by adsorbing reactive species in Zr–Al getter pumps, separating Ar from He and Ne by charcoal trap cooled at 77°K by liquid nitrogen. Noble gases analyses were performed using a sector-type mass spectrometer installed at noble gas laboratory of the INGV–Palermo.

He and Ne were then adsorbed and concentrated in another charcoal trap (cryogenic pump), cooled down at 12°K by a cold-head. This trap was strategically positioned close to the He mass spectrometer in order to concentrate each sample in a small volume (about few tens of cm^3) before expansion in the mass spectrometer, thus reducing the analytical error during analysis. A temperature controller allowed to separate the two species by releasing He at 40°K and Ne at 85°K, that were then separately admitted in a split flight tube mass spectrometer (Helix SFT) for isotope analysis. Ar previously adsorbed was finally released from the charcoal by heating the trap at room temperature and then admitted in a multi-collector mass spectrometer (Argus). Analytical error in air standard He isotope analysis was generally below 1%, while in Ar analysis was generally below 0.1%. The He and Ar abundances and isotope compositions were measured, as well the $^4He/^{20}Ne$ ratios, were determined in all of the investigated samples. During the experiments, typical He, Ne, and Ar blanks were negligible. The uncertainties in the noble-gases abundances were less than 10%.. The analytical results are listed in Table 5.1.

5. Helium and argon data

5.1 *Helium*

The chemical and isotopic compositions of noble gases from fluid inclusions provide direct evidence of the origin of magmatic fluids (e.g., Vityk et al., 1993; Moore et al., 2001; Boyce et al., 2003; Naden et al., 2003). Chemically inert noble gases can be used to trace the sources of trapped fluids, because their compositions are the result of physical processes such as mixing of fluids from several sources (mantle, crust, air, etc.).

As the gas extracted by the crushing technique produces a bulk sample resulting from many individual grains of differing densities and sizes of inclusions, noble gas abundances cannot easily be related to any magmatic process. For this reason, little importance is usually placed on the amounts of noble gases measured from FI bulk analysis.

Nevertheless, the good reproducibility of our data from various populations of crushed crystals of the same products indicates that abundances can yield estimates of the average contents of noble gases in magma. The table 5.1 lists helium and argon abundances and their isotopic ratios.

Fig. 5.1 shows that greater He abundances were measured in olivines and pyroxenes from the Marsili volcano and the ultramafic lava xenoliths of San Bartolo (Stromboli).

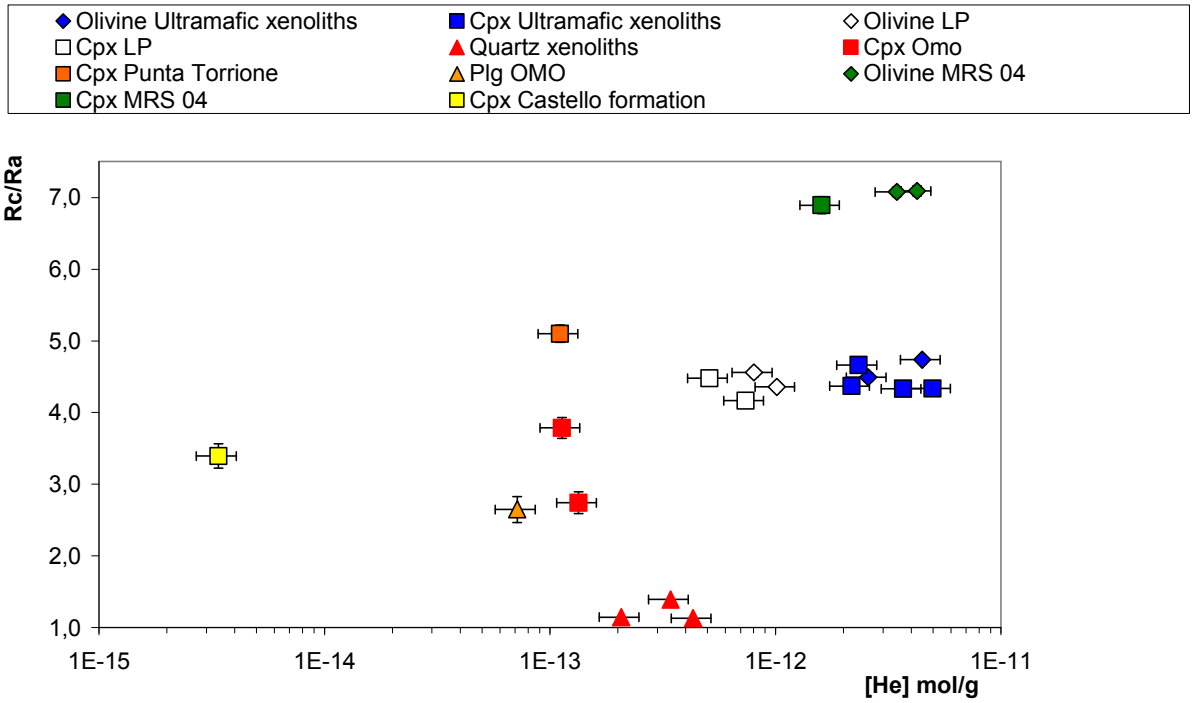

Figure 5.1- *He abundances vs. Ra/Rc crystals from the Marsili volcano, Panarea and Stromboli islands. The data of LP magma and ultramafic xenoliths from Martelli et al., 2010.*

Place	Sample	Mineral	[He]×10^{-13} mol/g	^{3}He/^{4}He (Rc/Ra)	Error %	[40Ar*]×10^{-13} mol/g	^{40}Ar/^{36}Ar	Error %	^{38}Ar/^{36}Ar	Error %	^{4}He/^{20}Ne
Marsili	MRS 04	ol	34	7.08	0.07	0.86	464.8	0.02	0.15	0.06	3203.74
Marsili	MRS 04	ol	42	7.09	0.072	0.341	304	0.02	0.18	0.06	1444.21
Marsili	MRS 04	cpx	16	6.89	0.119	0.64	363.3	0.02	0.19	0.06	709.97
Panarea	Castello formation	cpx	0.03	3.39	0.15	0.22	301.16	0.02	0.18	0.06	2.90
Panarea	Punta Torrione	cpx	1.1	5.1	0.12	0.032	304.02	0.02	0.12	0.06	16.79
Stromboli	HP	ol	0.25	0.53	0.06	0.35	301.5	0.02	0.02	0.06	3.95
Stromboli	HP	ol	0.09	n.d	n.d	0.49	307.78	0.02	0.14	0.06	n.d
Stromboli	HP	ol	0.01	n.d	n.d	0.029	298.94	0.06	0.20	0.27	10.2
Stromboli	HP	cpx	0.02	n.d	n.d	0.0095	320.34	0.02	n.d	n.d	1.70
Stromboli	Lp	ol	8	4,56	0.06	0.92	297.9	0.06	0.19	0.25	62.91
Stromboli	Lp	cpx	5	4,48	0.082	0.92	297.78	0.04	0.19	0.04	57.30
Stromboli	Lp	cpx	1.8	4,04	0.124	0.24	296.41	0.02	0.19	0.07	9.51
Stromboli	Lp	ol	10	4,36	0.057	1.22	296.53	0.02	0.20	1.05	108.88
Stromboli	Lp	cpx	7.4	4,16	0.091	1.10	298.31	0.02	0.19	0.06	20.66
Stromboli	Ultramafic xenoliths	ol	26	4,49	0.058	0.44	308.59	0.06	0.23	0.12	217.99
Stromboli	Ultramafic xenoliths	cpx	49	4,34	0.049	3.20	299.37	0.03	0.19	0.05	29.41
Stromboli	Ultramafic xenoliths	cpx	23	4,66	0.041	0.80	298.33	0.04	0.19	0.12	48.19
Stromboli	Ultramafic xenoliths	ol	12	4,36	0.108	0.45	298.96	0.30	0.19	0.06	11.29
Stromboli	Ultramafic xenoliths	ol	45	4,74	0.047	27	364.14	0.02	0.18	0.06	425.86
Stromboli	Ultramafic xenoliths	cpx	22	4,37	0.07	1.7	299.13	0.02	0.19	0.06	37.53
Stromboli	Ultramafic xenoliths	cpx	37	4,33	0.052	5.2	301.75	0.02	0.19	0.06	32.73
Stromboli	Quartz xenoliths	Quarz	2.1	1.15	0.046	36	350.25	0.02	0.19	0.06	1.48
Stromboli	Quartz xenoliths	Quarz	3.4	1.39	0.038	26	334.5	0.02	0.02	0.06	1.43
Stromboli	Quartz xenoliths	Quarz	4.3	1.13	0.029	7.6	328.95	0.02	0.19	0.06	0.85
Stromboli	Quartz xenoliths	Quarz	0.3	n.d		24	373.54	0.02	0.19	0.06	0.72
Stromboli	Quartz xenoliths	Quarz	0.1	n.d		3.7	338.16	0.02	0.19	0.06	0.48
Stromboli	Quartz xenoliths	Quarz	1.1	0.54	0.044	5.2	359.74	0.02	0.19	0.06	1.10
Stromboli	Quartz xenoliths	Quarz	0.77	0.72	0.035	17	385.65	0.02	0.18	0.06	0.67
Stromboli	Quartz xenoliths	Quarz	0.23	n.d		n.d	n.d		n.d		n.d
Stromboli	Cpx Omo	cpx	1.1	3.78	0.15	0.071	298.64	0.02	0.20	0.06	11.52
Stromboli	Cpx Omo	cpx	1.33	2.74	0.15	n.d	n.d		n.d		25.5
Stromboli	Plg Omo	plg	0.72	2.65	0.18	0.23	297.85	0.02	0.19	0.06	1.46

Table 5.1 - *Noble-gas abundance and isotope ratios in the investigated minerals . n.d.: not determined. The data of LP magma and ultramafic xenoliths from Martelli et al., 2010.*

He abundances from Marsili were 3.45-4.24 (× 10^{-12} mol/g) and 1.6 (× 10^{-12} mol/g) in olivines and pyroxenes, respectively. The data from Stromboli varied widely from 1.62 (× 10^{-15} mol/g) to 4.97 (×10^{-12} mol/g) in pyroxene and from 8.76 (×10^{-15} mol/g) to 4.47 (×10^{-12} mol/g) in olivine. The greater He abundances in the xenoliths ultramafic San Bartolo lavas with respect to all the other samples from Stromboli may be explained by their greater formation pressure (P > 0.65-1.1 Gpa, equivalent to a depth of 19-33 km, Laiolo and Cigolini, 2006; Cigolini et al., 2008). The low gas content of HP products meant that their chemical concentrations could be measured, but not their $^3He/^4He$ ratios (^3He could not be detected in HP products, since it was from 10^5 to 10^6 times less abundant than ^4He). The situation was similar at Panarea, where highly degassed magma and small quantities of He in samples meant that neither abundances nor $^3He/^4He$ isotopic ratios could be measured. This was only possible in two pyroxene samples from Punta Torrione ("brown tuff" in the literature) and Punta del Tribunale (Castello formation).

The rocks from Panarea are compositionally variable in terms of major elements, trace elements and isotopes - the result of several processes, including supergene alteration. The products interact with the extensive gaseous exhalations and low-pH fluids released over the area. The originally andesitic-dacitic composition of the local volcanic products have been variously altered to argillic hydrothermal facies. A well-developed system of fractures and faults enhanced the circulation of hydrothermal fluids inside the volcanic rocks. XRD analyses show the typical mineralogical composition of volcanic rocks (alunite, jarosite, kaolinite, quartz) altered by an acidic environment.

A separate discussion is reserved for the He and Ar abundances in quartzite nodules hosted by calc-alkaline lava of the Paleo-Stromboli II period (Omo lavas).

Table 5.1 lists, also, the $^4He/^{20}Ne$ ratios of all samples. $^3He/^4He$ ratios were corrected for air contamination according to $^4He/^{20}Ne$ ratios and expressed as Rc/Ra, the former being the $^3He/^4He$ ratio in air, and the latter the corrected ratio. At Marsili, the Rc/Ra ratios vary in the range 7.07-7.09 in olivine and 6.89 in pyroxene, and these values are the highest found in the Mediterranean basin, together with R/Ra ratios measured in peridotite mineral phases from the Hyblean Plateau (Sapienza et al., 2005), Mt. Etna (Nuccio et al., 2008) and the volcano of Alicudi (Martelli et al., 2008). The He isotopic composition of Marsili (~7 Ra) is the highest in the region, and implies that crustal fluids did not significantly modify the He isotopes of the mantle source. According to Trua et al. (2010), sample MRS 04 approaches typical MORB values, due to its high CaO content in the host olivine and the high CaO/Al_2O_3 ratio of the melt inclusions.

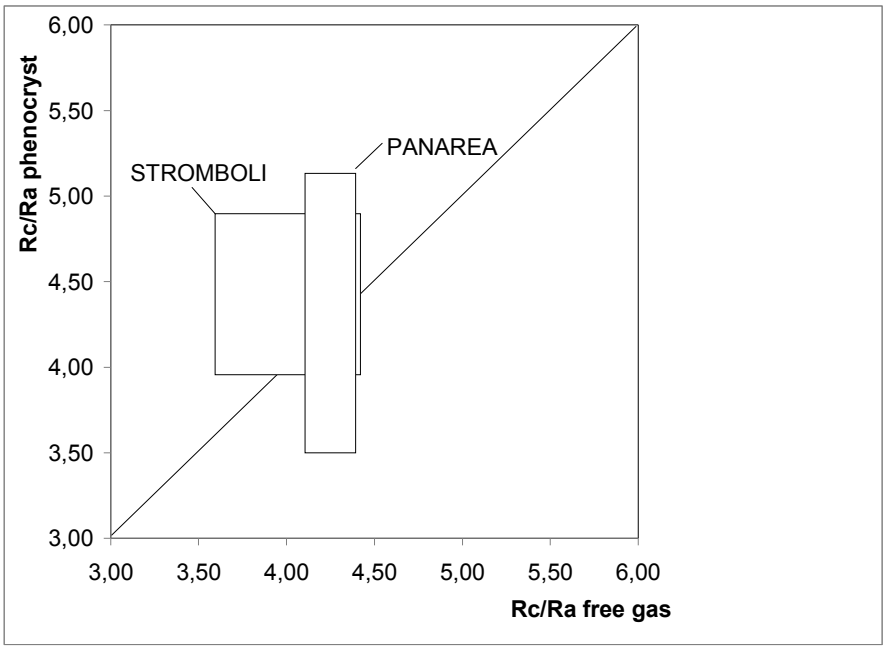

Figure 5.2- *A comparison of the $^{3}He/^{4}He$ of phenocryst-hosted fluid inclusions with $^{3}He/^{4}He$ of free gases from the same volcanic district. Free gas data are from Stromboli (Inguaggiato and Rizzo, 2004) and Panarea (Caliro et al., 2004).*

At Stromboli, He isotopic ratios in free gases and thermal waters match data from fluid inclusions in olivine and pyroxene (fig. 5.2). This shows that the isotopic signature is maintained as the gas ascends toward the surface, confirming that the maximum $^{3}He/^{4}He$ ratio of fluids generally reflects degassing of magmatic bodies at depth (Martelli et al., 2004). The $^{3}He/^{4}He$ ratios vary in the ranges 3.70-4.66 for pyroxene and 4.36-4.74 for olivine. The He isotope data therefore indicate that pyroxene from the Omo lava has lower Rc/Ra values than that of LP magma and the San Bartolo ultramafic xenoliths. Samples having similar $^{4}He/^{20}Ne$ ratios contain a similar percentage of air (Sano and Wakita, 1985). Since the pyroxene of the Omo lava has a $^{3}He/^{4}He$ ratio lower than those of LP magma, for the same $^{4}He/^{20}Ne$ ratio (Fig. 5.3), air contamination cannot be the main process responsible for the observed differences in Rc/Ra values. This difference may be explained by degassing at shallow depths, which would induce progressive ^{3}He depletion in the magma during vesiculation (Nuccio and Valenza 1998). As magma rises through the volcanic conduit, pressure decreases, and the magma reaches volatile saturation and begins to exsolve gases into bubbles. According to Nuccio and Valenza (1998), if magma depressurization develops rapidly, He isotopes may undergo kinetic fractionation, because ^{3}He diffuses into the growing bubbles faster than ^{4}He, so that the magma progressively becomes depleted in ^{3}He. This process can be modeled by Rayleigh's distillation. The two samples from Panarea display very different $^{3}He/^{4}He$ ratios and helium abundances. The

Castello formation sample is very low in He, and has a $^{3}He/^{4}He$ ratio of 3.39 Ra, whereas the Punta Torrione samples have abundant He, with values similar to those of the Stromboli lava pyroxene, which has a $^{3}He/^{4}He$ ratio of 5.1 Ra, like that measured at Salina and Vulcano (Martelli et al., 2008). These flows belong to different volcanic series, and are interpreted as deriving from different mantle sources. The Punta Torrione flow belongs to the calc-alkaline basalt series which is similar in composition to the western arc, whereas the Castello flow is geochemically similar to that of Stromboli (Calanchi et al., 2002). Lucchi et al. (2010) have recently suggested that the source of brown tuff is located beyond Panarea, within the La Fossa Caldera of Vulcano.

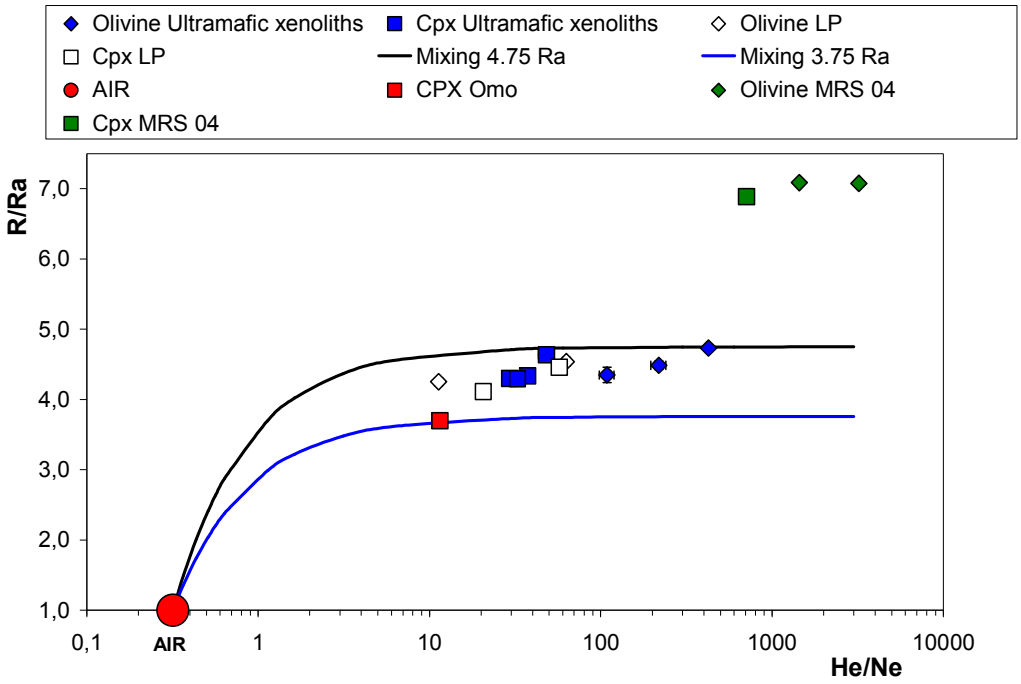

Figure 5.3 - *Uncorrected R/Ra versus He/Ne molar ratios scatter plot. All samples, are variably contaminated by air ($^{4}He/^{20}Ne_{air}$ =0.318; $^{4}He/^{20}Ne_{a.s.w.}$ =0.285). Olivine and pyroxene plot on a mixing curve between air and a magmatic end-member with R/Ra = 4.75 and 3.75.*

Fig. 5.3 plots the $^{3}He/^{4}He$ ratios, uncorrected for air contamination, versus $^{4}He/^{20}Ne$ ratios. Note the clear-cut contribution of upward-moving air from olivine to pyroxene.

At Stromboli, a trend of mixing with air exists (confirmed by $^{40}Ar/^{36}Ar$ between 296 and 360), but it does not significantly affect $^{3}He/^{4}He$ ratios. The curves represent the theoretical mixing lines between air and two possible end-members at 4.75 and 3.75 Ra. Exactly how this contamination occurred is debated, and two alternative processes have been considered to explain it:

1. The Stromboli magmas were contaminated by fluids with an atmosphere-like signature in the shallow system. Generally, the $^{4}He/^{20}Ne$ ratios of pyroxene are lower than those of olivine, especially in the ultramafic xenoliths, which may indicate a larger fraction of atmospheric neon in pyroxene, which crystallizes after olivine. The process is less clear for LP products, in which the $^{4}He/^{20}Ne$ ratio is sometimes higher in pyroxene than in olivine.

   Di Carlo et al. (2006) suggest that clinopyroxene precedes olivine in the crystallization sequence and persists as the liquidus phase down to at least 200 Mpa. This may explain the $^{4}He/^{20}Ne$ ratio measured in the volatile-rich high-K basalt from the recent eruptive activity of Stromboli;
2. In their hypothesis on the origin of this atmospheric component, Nuccio et al. (2008) report that microscopic inspection of the crystals reveals that most of them have a number of microcracks connected with the surface, and propose that they trap air during eruptive activity or later. Such entrapped air can be released easily only when the crystals are crushed and the microcracks are exposed. Clearly, as a given atmospheric contribution causes more significant effects when added to smaller amounts of gas, it is not surprising that this phenomenon is more evident in products containing the smallest amounts of gas.

The origin of the HP shallow magma is mainly attributed to discrete intrusions of deep LP magma into shallow reservoir and its mixing with the residing HP magma (Francalanci et al., 1999; Landi et al., 2004). This induces mineral phase dissolution, followed by crystallization, mainly driven by water loss at low pressure (Métrich et al., 2001; Landi et al., 2004; Francalanci et al., 2005). Continuous mixing between these two magmas has been clearly documented in several textural, mineralogical, chemical and isotopic studies (Francalanci et al., 1999, 2004, 2005; Landi et al., 2004, 2006, 2008b; Armienti et al., 2007). The shallow magma system is also affected by significant recycling of crystals deriving from old cumulus crystal mushes (perhaps up to 10 ka in age) situated just below the volcanic edifice, as indicated by isotope studies on bulk rocks and in situ Sr isotope microanalysis (Francalanci et al., 2005).

The refilling magma batches derive from volatile-rich parental melts via crystal fractionation, at a lithostatic pressure of 200–300 MPa, corresponding to a depth of ~7.5–11 km, as determined from H_2O and CO_2 contents dissolved in melt inclusions within olivine in LP pumice (Métrich et al., 2001, 2005; Bertagnini et al., 2003).

According to Vaggelli et al. (2003) and Francalanci et al. (2004, 2005), mixing between HP and LP magmas, concomitant with continuous crystallization of olivine, pyroxene and plagioclase, occurs in an intermediate reservoir at a depth of ~3 km, probably the remnant of an old Stromboli structure. Continuous refilling of the shallow magma body from depth, together with concomitant magma emission, determines the steady state of the plumbing system (Landi et al., 2008a). Given that mingling exists, Martelli et al. (2010) have demonstrated that the $^3He/^4He$ values measured in LP are not influenced by HP helium released during crushing. Assuming a hypothetical $^3He/^4He$ ratio of HP = 3 Ra, they show that the LP values are not influenced by HP contributions (Fig. 4.4).

$$^3He/^4He_{fin} = \frac{^3He/^4He_{HP} * [He]_{HP} * X_{HP} + {}^3He/^4He_{LP} * [He]_{LP} * (1-X_{HP})}{He_{HP} * X_{HP} + He_{LP} * (1-X_{HP})}$$

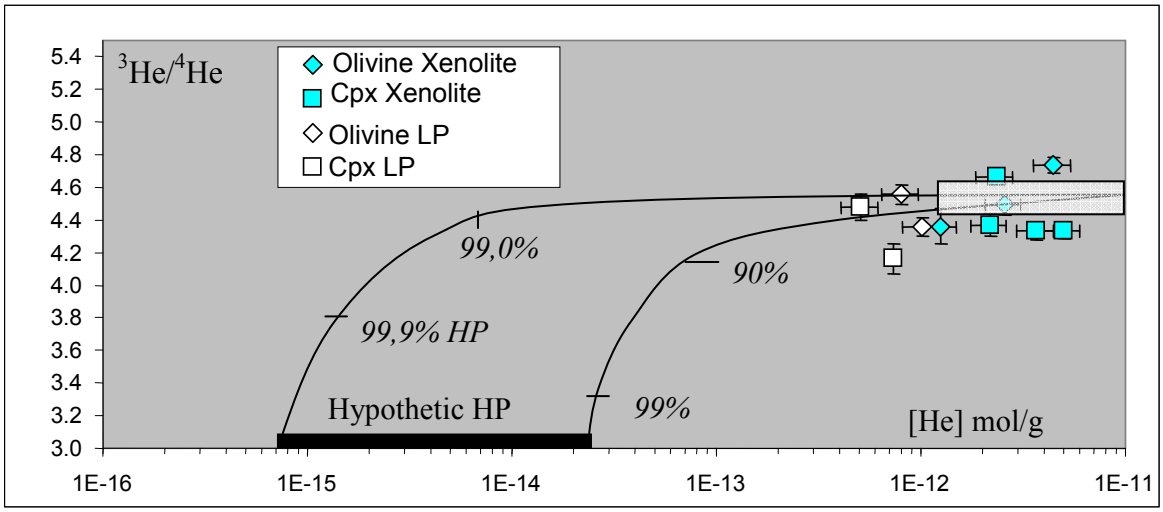

Figure 5.4 *– Mixing of a hypothetical $^3He/^4He$ ratio of HP with LP magma; data from Martelli et al. 2010.*

5.1.1 Cogenetic olivines and pyroxenes

In Fig. 5.5 all the studied pairs of cogenetic olivines and pyroxenes are plotted against their respective $^3He/^4He$ ratios, expressed as Rc/Ra. These ratios are generally lower than MORB values (8±1 Ra), except for sample MRS 04 (Rc/Ra 7.09). Basalts with $^3He/^4He$ lower than the southern Italian maximum (~7 Ra) contain radiogenic He. In the prevailing hypothesis, this is derived from the mantle wedge (Martelli et al., 2004). However, crustal contamination of magma prior to eruption has occasionally been recorded in southern Italian volcanism (Ellam and Harmon, 1990; De Astis et al., 2000).

Of the six cogenetic olivine and pyroxene phenocrysts, five pyroxene samples have lower $^{3}He/^{4}He$ than the olivine ones. This may indicate subtle crustal contamination, and pyroxene $^{3}He/^{4}He$ measurements can consequently only be considered as a lower limit on the magmatic value.

The generally lower $^{3}He/^{4}He$ ratios found in clinopyroxene compared with olivine may be broadly interpreted in at least four ways:

1) clinopyroxene postdates olivine traps helium later, within a parent magma having a decreasing $^{3}He/^{4}He$ ratio;
2) lower $^{3}He/^{4}He$ ratios in clinopyroxene may be the result of a lower effective closure temperature. The pyroxenes continue to exchange helium with the magma after the olivines had closed (Marty et al., 1994; Hilton et al., 1995);
3) helium isotopes are affected by mass-dependent fractionation throughout the crystal lattice (Harrison et al., 2004). This may occur during helium diffusion from phenocrysts within sub-solidus magma;
4) helium isotopes undergo mass-dependent fractionation during bubble exsolution and degassing.

All these possibilities explaining the disequilibria among the above cogenetic minerals may be considered valid for the case in question, as no clear position can currently be stated with respect to one hypothesis or another.

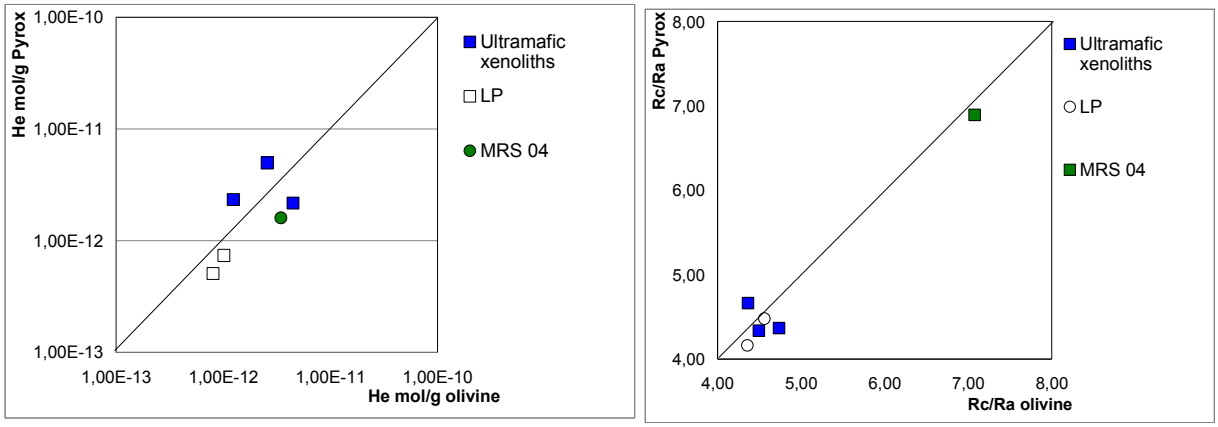

(a) **(b)**

Figure 5.5 - *Comparison of He concentration values (a) and of Rc/Ra values (b) between cogenetic olivine and clinopyroxene.*

5.2 Argon

Fig. 5.6 shows the $^{40}Ar/^{36}Ar$ versus $^{4}He/^{20}Ne$ ratios of the samples. The measured $^{40}Ar/^{36}Ar$ ratios fall in the range of subduction-related volcanism, well below typical mantle values (Burnard et al., 1997; Fischer et al., 2005), and close to the atmospheric signature. At Stromboli and Panarea, olivine and pyroxene have low $^{40}Ar/^{36}Ar$ ratios,

varying in the range 296-360 at Stromboli and 301-304 at Panarea, close to the atmospheric signature ($^{40}Ar/^{36}Ar$ = 295.5). At Marsili, the $^{4}He/^{20}Ne$ ratios of all samples showed high values ($^{4}He/^{20}Ne$ > 3000 in olivine), suggesting low atmospheric contamination, according to the highest measured values of $^{40}Ar/^{36}Ar$ (363-465).

It should be noted that the $^{40}Ar/^{36}Ar$ ratios in quartz xenoliths are higher than those for air (295.5) but much lower than MORB values ($^{40}Ar/^{36}Ar$ > 40000; Burnand et al., 1997), supporting the hypothesis that fluids were released by a basaltic magma, partly trapped as fluid and melt inclusions, in accordance with the model in which partial melting of crustal rocks occurred in the middle-lower crust, forming rhyolitic melts + CO_2 fluids (Zanon et al., 2003).

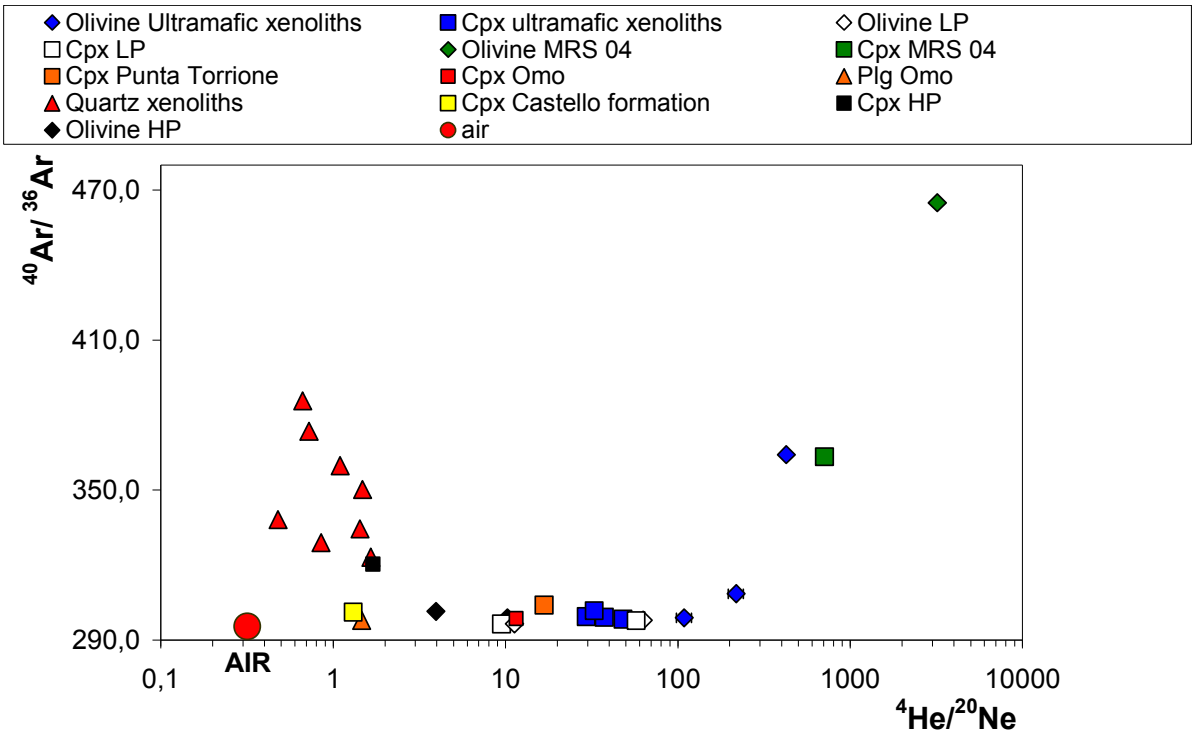

Figure 5.6 - *$^{40}Ar/^{36}Ar$ versus $^{4}He/^{20}Ne$ ratios of the all samples. In the plot is reported the air value for $^{40}Ar/^{36}Ar$ and $^{4}He/^{20}Ne$ ratios.*

To rule out possible air contamination, all ^{40}Ar data were corrected for atmospheric contamination on the basis of ^{36}Ar abundances, assuming that ^{36}Ar dissolved in magma is negligible:

$$^{40}Ar^{*} = {}^{40}Ar_{observed} - {}^{40}Ar_{air}$$

where: $^{40}Ar_{air} = (^{40}Ar/^{36}Ar)_{air} \times {}^{36}Ar_{observed}$

$^{40}Ar/^{36}Ar$ versus Ar* values confirm atmospheric contamination for the Stromboli and Panarea samples and, low air contamination for the Marsili samples. They also emphasize the high content of argon in the fluid inclusions hosted in quartz xenoliths (Fig. 5.7).

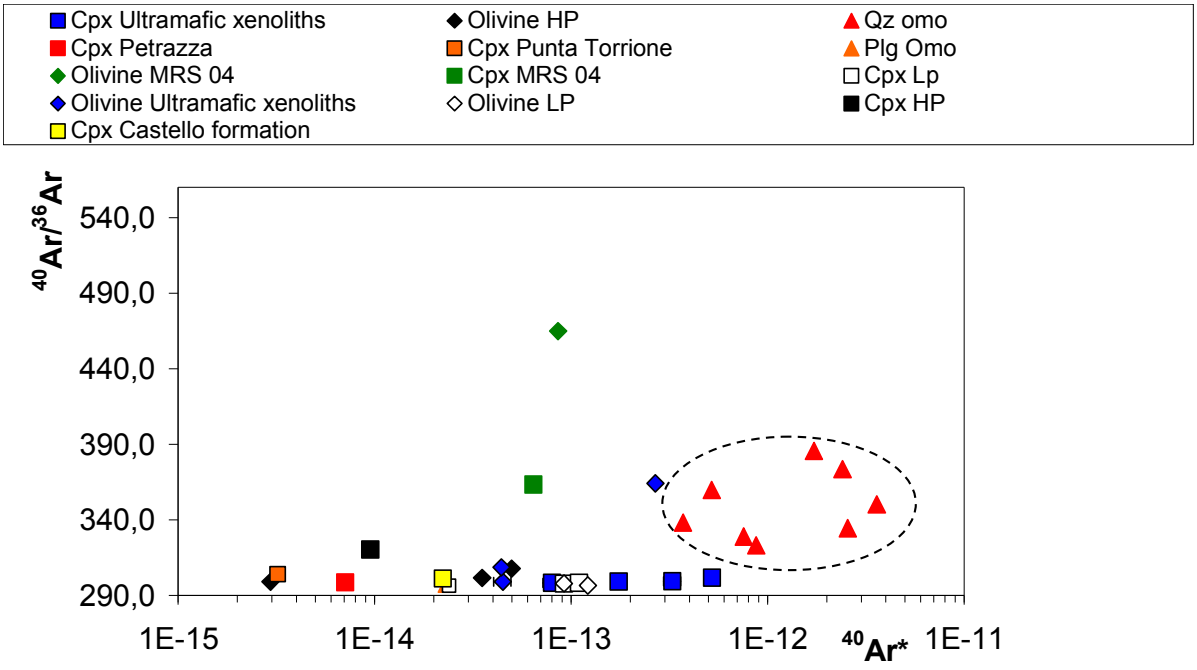

Figure 5.7- *$^{40}Ar/^{36}Ar$ vs. Ar* diagram in mineral samples investigated. The dotted curve contains the samples of quartz xenoliths.*

5.3 Diffusion of Helium and Argon in quartz xenoliths

As inclusion fluids may be trapped both at the time of formation of host minerals and after it, their chemical and isotopic compositions can provide unique insights into the evolution of fluid compositions over time. Noble gases can be transported and fractionated by diffusion, and the lighter noble gases are expected to be the more active in this respect. Diffusion has been extensively discussed as a reason for retention of noble gases within individual minerals, especially in the context of age estimates. On a larger scale, several diffusion paths are possible, e.g., diffusion along grain boundaries, which may affect large-scale transport. However, as obtaining coefficients for such pathways by experiment or in the field is problematic, such a process is sometimes hypothesized but cannot be quantitatively evaluated. Diffusion clearly provides the potential for generating isotopic variations as well, although this has not been widely documented, since many silicate phases may be open to noble gas loss by diffusion at elevated temperatures but not at lower

ones. Current mechanistic understanding of solid-state diffusion of noble gases through crystalline materials is based on limited experimental results. Measurement of diffusion coefficients typically entails direct determination of concentration profiles following inward diffusion (charging experiments; e.g., Watson and Cherniak, 2003) or, more commonly, measuring gas release during step-heating of samples with either natural or artificially added diffusant (degassing experiments; e.g., Fechtig and Kalbitzer, 1966; Dunai and Roselieb, 1996; Farley, 2000; Shuster et al., 2004). Several studies have been carried out on the kinetics of noble gas diffusion inside silicate minerals, olivine and pyroxene, but diffusion kinetics in quartz minerals have not yet been well characterized (Masarik et al., 2001a; Niedermann, 2002). The works of Trull et al. (1991), Watson and Cherniak (2003) and Shuster and Faerley (2005) yield information on the various trends of diffusion coefficients according to temperature for He in quartz and olivines, and for Ar in quartz (Fig. 5.8). The Arrhenius plot shows that the trends of He and Ar with temperature are linear, in both quartz minerals and olivine, revealing different diffusion parameters for each element. In particular, the diffusion coefficients calculated by Trull et al. (1991) for He in olivine and quartz differ. Temperature being equal, the diffusion coefficients of He in quartz are higher than those of olivine (logD:10^{-6}> 10^{-10} at 1000°C), fitting the low He measured in quartz xenoliths with respect to the olivine of all samples (Fig. 5.8).

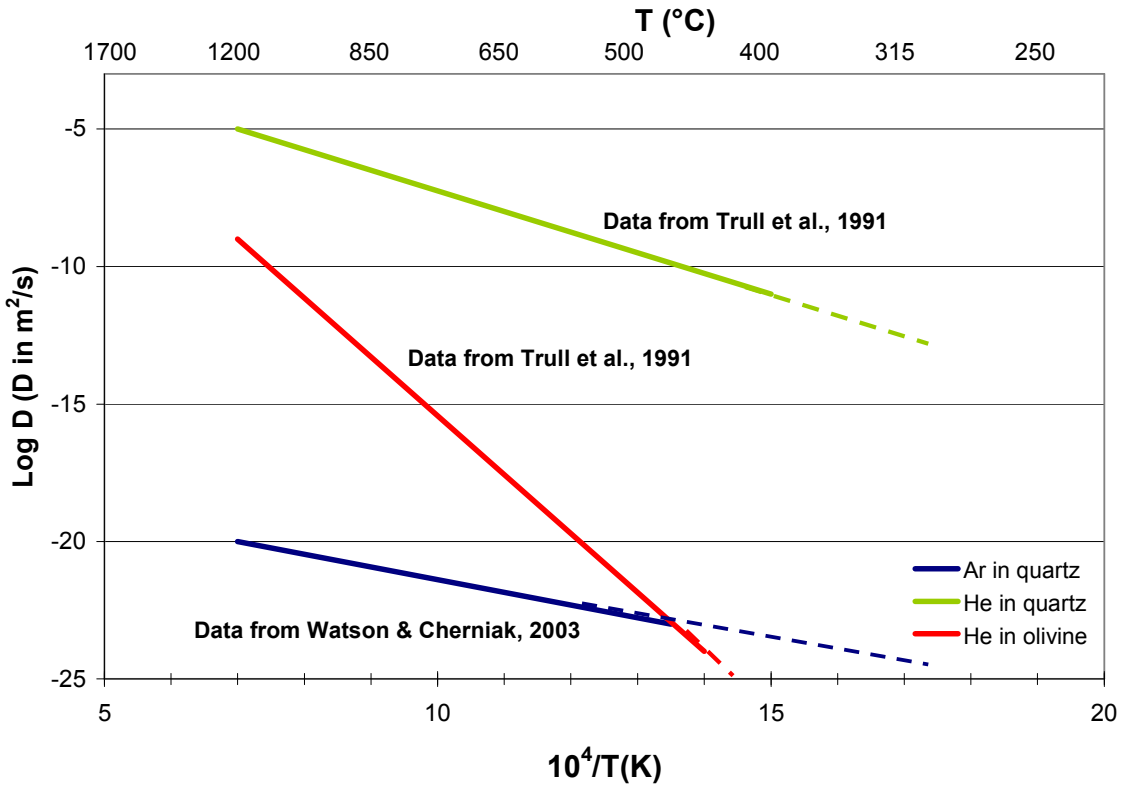

Figure 5.8- *Arrhenius plot shows trends of He and Ar with temperature in quartz and olivine.*

Fig. 5.8 also shows that the calculated Ar diffusion coefficients (D) in mineral quartz are lower than those of He at the temperatures, between 1200 and 300 °C.

The Ar diffusion coefficients measured by Watson and Cherniak (2003) perfectly match the data in Fig. 5.9, showing He versus Ar* abundances.

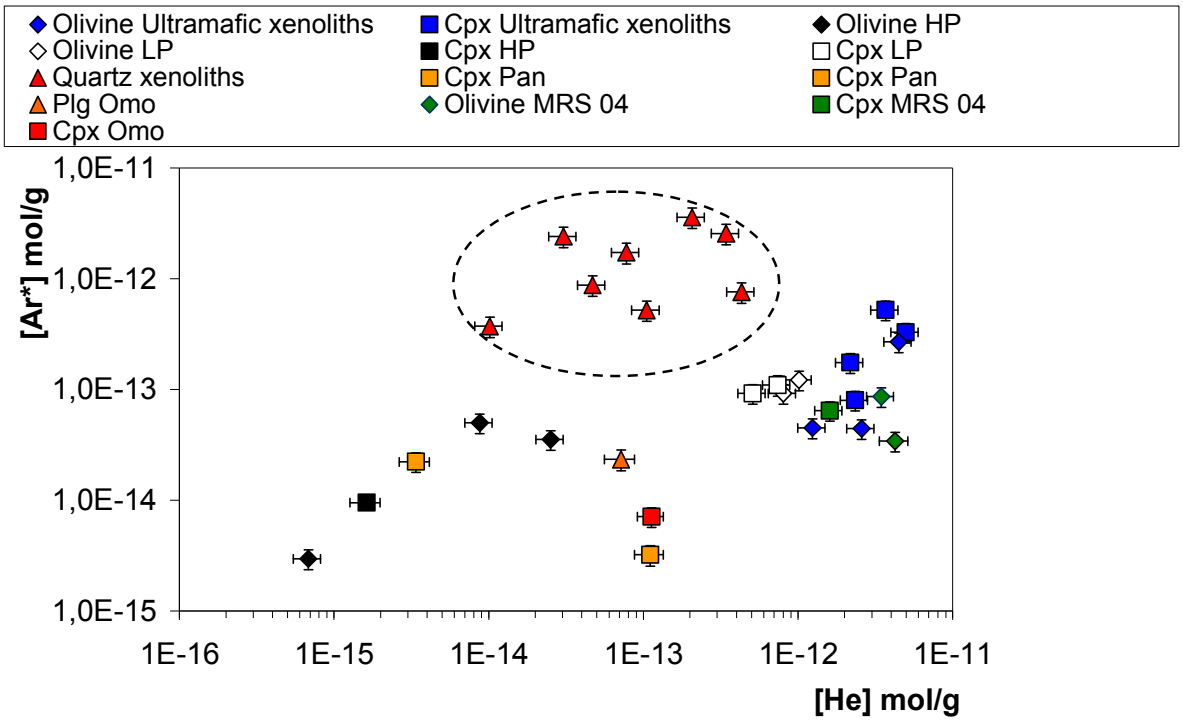

Figure 5.9 – *He vs Ar* abundances diagram in all samples. The dotted curve contains the samples of quartz xenoliths.*

It is clear that the Ar abundances measured in quartz xenoliths are comparable to or more abundant than those of the olivine and pyroxene of all samples. Fig. 5.10 shows that low Rc/Ra values correspond to high Ar*. These data match the high values of $^{40}Ar/^{36}Ar$ measured, showing that diffuse, selective loss of He with respect to Ar is the prevailing process, so that atmospheric contamination is a secondary process. Thus, the low values of Rc/Ra in the quartz xenoliths are due to loss of He by diffusion. The Rc/Ra versus He/Ar* graph (fig.5.11) also confirms this hypothesis. The above figures confirm the observations of Watson and Cherniak (2003) as regards the diffusion of Ar in quartz, which is lower than that of He.

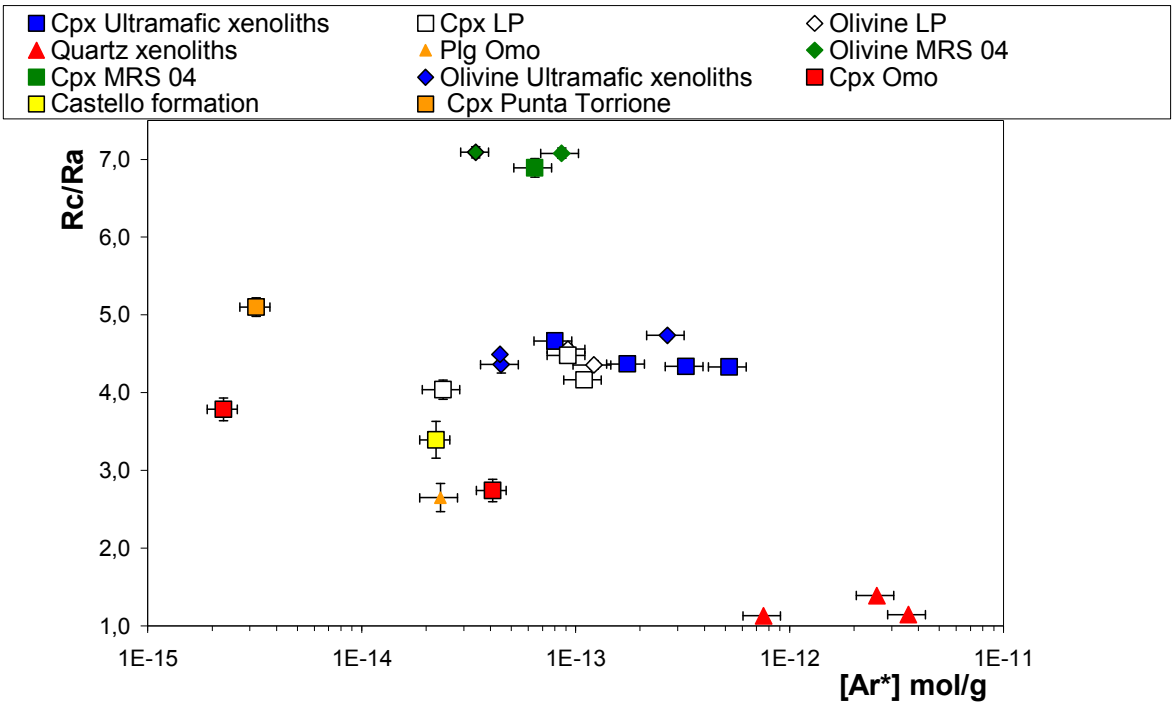

Figure 5.10- *He isotope ratios vs Ar* abundances diagram in all samples.*

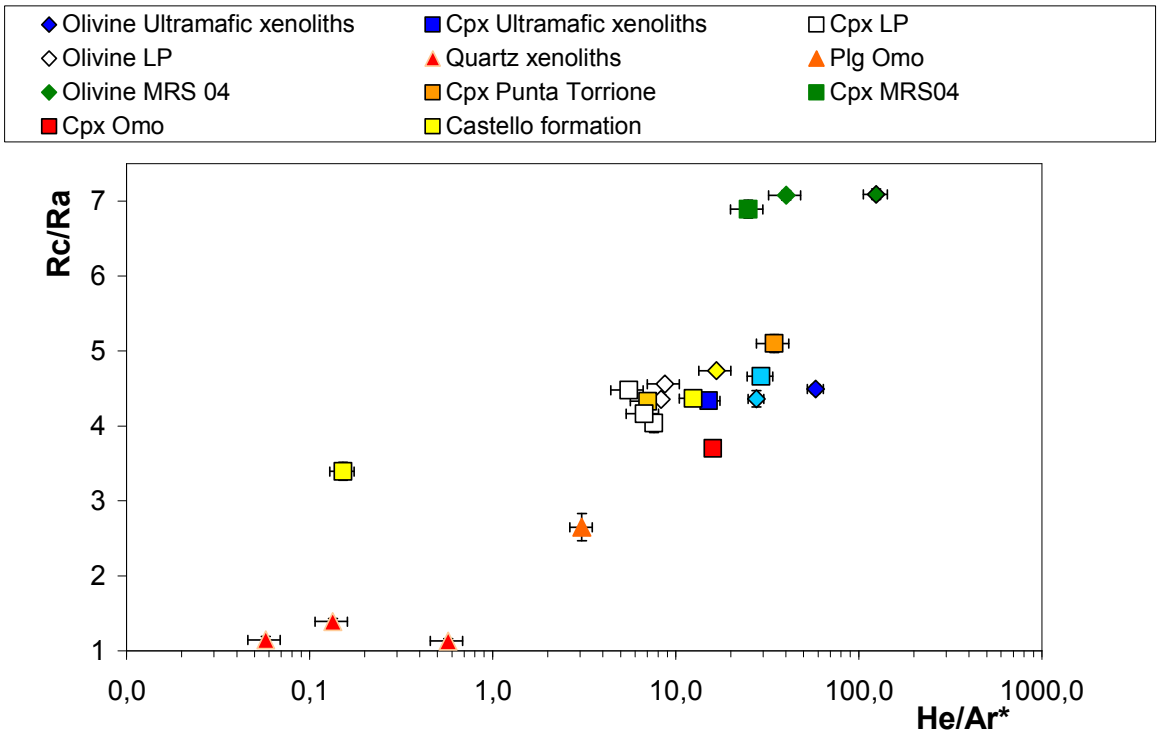

Figure 5.11- *He isotope ratio vs Ar* scatter plot in all samples.*

The above authors also state that crystal density affects diffusion coefficients, particularly those of olivine and quartz, which are 3.27 and 2.65 g/cm^3, respectively. These values imply a ranking of structural openness, or ionic porosity, in the order quartz > olivine. It is also useful to know that Ar atoms are ~70% larger than He ones. The observed slow diffusion of Ar with respect to He in the quartz studied by Watson and Cherniak (2003) is reasonable, simply because of the difference in size of the atoms. These considerations also fit the hypothesis of Vaggelli et al. (2003) on the origin of quartzite nodules and their formation pressure. These authors interpret the restitic product of a partial melting process as involving felsic metamorphic rocks surrounding the deepest magmatic reservoir, and crustal rocks such as "felsic granulite/orthogneiss" are assumed to occur below Stromboli at a depth of about 11 km. The fact that the Stromboli magma led to the formation of restitic quartzite has significant implications with regard to magma evolution processes, because it is direct evidence of crustal contamination.

5.4 *Interference of magmatic source*

The $^3He/^4He$ ratios measured in the olivine and pyroxene from Marsili are similar to those measured at Pantelleria, Etna, the Hyblean plateau and the volcano of Alicudi (~ 7 Ra). Although all these volcanoes derived from a variety of tectonic regimes (subduction-related, intraplate, rifting), their similarities suggest the common origin of their geochemical features. Their characteristics are consistent with a HIMU-like mantle (high U/Pb). The $^3He/^4He$ ratio of the HIMU end-member is (6.8 ± 0.9 Ra, Hanyu and Kaneoka, 1997; Moreira and Kurz, 2001).

The ratios of helium and argon isotopes from mafic volcanic rocks from the Marsili volcano does not allow us to discriminate the source mantle beneath the most recent basin of the Southern Tyrrhenian back-arc basin, although we can certainly state that the mantle composition was little affected by subduction-related metasomatism.

Recent studies (Trua et al., 2010) show that the melt inclusions of sample MRS 04 have relatively flat normalized trace element patterns, which is not observed in the other Marsili whole rocks, but which broadly overlap the field of the N-MORB bulk rock samples recovered from the nearby Vavilov back-arc basin. The discovery of these melt inclusions documents the existence of MORB melts beneath the Marsili back-arc basin, hitherto not identified by whole rock analyses of its lavas. Analyses of fluid inclusions of the olivine

and pyroxene of sample MRS 04 may support the remarks of the above authors on the presence of a MORB-type mantle component in the samples from Marsili.

The low He isotope ratios of basalts from the eastern Aeolian Islands are typical of subduction zones. The absence of radiogenic He in oceanic-arc basalts and fluids suggests that the direct addition of radiogenic He by subduction of oceanic lithosphere is unlikely (Patterson et al.,1994; Dodson and Brandon, 1999; Bach and Niedermann, 1998; Hilton et al., 2002). The presence of radiogenic He in the Plio-Quaternary basalts of Italy therefore relies on a continental source. The presence of subducted continental crust in Italy is well documented (e.g., Carminati et al., 2005).

The isotope trace element signature of Italian back-arc basalts supports contamination of the mantle wedge by fluids derived from subducted crustal rocks (Gasperini et al., 2002; Peccerillo, 2005). The radiogenic He in the mantle wedge may originate from two sources: (1) He ingrowth in the mantle wedge after metasomatic enrichment by U and Th, and/or (2) addition of crustal radiogenic He to the mantle wedge via fluids from the subducted slab. The effect that both processes have on altering the isotopic composition of mantle He strongly depends on the initial concentration of the unmodified mantle. Admittedly, this is a poorly constrained parameter, as the depleted MORB-mantle (DMM) source has a relatively well-established He concentration ($1.5 \times 10^{-5} cm^3 STP/g$) (Allegre et al., 1986/1987; Sarda and Graham, 1990). The duration of the ingrowth of ^4He due to metasomatic addition of U and Th from the slab is limited. Westward subduction of the Ionian-Adria micro-plate started no earlier than 30 Ma ago (Doglioni et al., 1999), providing an upper limit.

The metasomatized mantle has maximum contents of 200 ppm U and 950 ppm Th, producing 1.5×10^{-6} cm^3 STP $^4He/g$ in 30 Ma (Martelli et al., 2004). This is sufficient to reduce the $^3He/^4He$ of a DMM source (typically 7–9 Ra) by less than 10%, and cannot explain the low ratios of Italian basalts. Post-metasomatic He ingrowth could only decrease mantle $^3He/^4He$ significantly if the initial He mantle concentration were two orders of magnitude or less than the DMM concentration. For radiogenic He in the Italian basalts to originate in subducted continent-derived material, a mechanism to transport crustal He to the fluids metasomatizing the mantle wedge is required. Of the common rock-forming minerals, garnet probably has the highest closure temperature (Tc = 600°C; Dunai and Roselieb, 1996) and could transport crustal radiogenic He to the greatest depths. It is worth noting that, if the Tc of He in garnet is as low as the value proposed by Blackburn and Stockli (2006) (110–300°C), He would not be transported to significant depths.

In order to assess the maximum amount of He that could be transferred to the mantle wedge above the subducting slab, we assume that all the He produced in the garnet of the crustal basement is entirely transferred to the wedge via an aqueous fluid or melt.

Therefore, neither post-metasomatic ingrowth nor the direct addition of crustal He can explain the low $^{3}He/^{4}He$ mantle prevalent in Italian magmatism, if it started with DMM He concentrations. A mantle reservoir with a He concentration low enough for either mechanism to have generated radiogenic $^{3}He/^{4}He$ would rapidly evolve into low $^{3}He/^{4}He$ (unless buffered by additional He from elsewhere). It is very unlikely that a low (He) HIMU mantle reservoir could consistently evolve the remarkably constant $^{3}He/^{4}He$ ratio which is typical of the global HIMU mantle source (Hanyu and Kaneoka, 1997). It is more probable that mantle He was lost as a result of metasomatism. One mechanism may be that percolation of metasomatic fluids devolatilizes the mantle wedge in a manner similar to that during aqueous/carbonic fluid infiltration through crustal rocks (Bickle and Baker, 1990).

As regards the origin of the quartzite nodules, the literature reports that they also occur in other volcanoes of the Aeolian Arc (e.g. Filicudi, Alicudi, Salina,Vulcano), where they appear to have a similar origin (Francalanci and Santo 1993; Peccerillo et al. 1993; Zanon 2001; Frezzotti et al. 2002). This indicates that crustal contamination is a common process occurring in most of these volcanoes, and may be responsible for a typical characteristic of the Aeolian magmas, i.e., the steeper evolutionary trends of the magmatic series, crossing the borderlines between various fields in the K_2O vs. silica classification diagram (Francalanci 1997, and references therein).

Quartzite nodules at Stromboli are found only in the calc-alkaline lava of Strombolicchio and PSTII. Previous studies have reported the occurrence of felsic nodules in Strombolicchio since the late 19th century (Johnston-Lavis 1893). Honnorez and Keller (1968) suggest that they are metamorphic in origin, due to contacts between sedimentary rocks and calc-alkaline lava. Pezzino and Scribano (1989) describe two types of quartzite nodules: the first of sedimentary origin from quartzite, and the second of metamorphic origin from the Hercynian Calabro-Peloritano basement. Their petrographic characteristics indicate that they represent restitic rocks produced by partial melting of crustal rock. The almost exclusive presence of quartz is interpreted as the result of melting, when quartz remained as a residual phase. The abundance of argon (2.94 to 23 $\times$ 10^{-12} mol/g) and the high $^{40}Ar/^{36}Ar$ ratio (323-385) of the quartz xenoliths analysed in the present study confirm this hypothesis since, in agreement with Zanon et al. (2003), fluids released by basaltic

magma during partial melting of crustal rocks are partly trapped in fluids and melt inclusions.

The presence of quartzite nodules only in calc-alkaline rocks of significantly different ages is interpreted by Vaggelli et al. (2003) as due to their density or, more probably, to their short residence time in reservoirs and/or fast upwelling. Calc-alkaline magma does have a constant, quite primitive composition, indicating its rather rapid transit through the continental crust. Fast upwelling has also been suggested on the basis of fluid-inclusion evidence in quartzite nodules Vaggelli et al. (2003). It may therefore be hypothesized that, in the case of longer magma residence time, xenoliths are completely digested by assimilitation+fractional crystallization. These processes lead to increasing contents of potassium, incompatible trace elements and silica and higher Sr isotope ratios in the host magma, thus generating more evolved and Sr radiogenic magma with a different serial affinity (e.g., high-K andesites of PST I). The general evolution of Stromboli therefore involved processes which also occur in the other volcanoes of the Aeolian Arc, which are similarly characterized by several compositional variations in rocks which occurred over a short period of time. The presence of felsic metamorphic rocks affected by partial melting processes in the basement may also be evidence which can be extended to the rest of the Aeolian Arc.

6. CONCLUSIONS

Noble gas analyses on phenocrysts from volcanic rocks from the islands of Panarea and Stromboli and the volcano of Marsili were carried out to evaluate the origin of magmatic fluids in the southern Tyrrhenian basin.

Helium isotopes in phenocrysts from volcanic rocks from the Aeolian Islands and Marsili have inhomogeneous $^{3}He/^{4}He$ ratios.

Analyses of fluid inclusions of the olivine and pyroxene of sample MRS 04 may support the remarks of Trua et al. (2010) on the presence of a MORB-type mantle component in the samples from Marsili, although a HIMU-type source may be hypothesized to explain the isotopic ratios of He and Ar.

The He and Ar isotopic ratios from mafic volcanic rocks from the Marsili volcano cannot discriminate the mantle source under the most recent back-arc of the southern Tyrrhenian basin, although the mantle composition was definitely only slightly affected by subduction-related metasomatism.

The $^{3}He/^{4}He$ ratios measured in the olivine and pyroxene from Marsili are similar to those measured at Pantelleria, Etna, the Hyblean plateau and the volcano of Alicudi (~7 Ra). Although all these volcanoes derived from a variety of tectonic regimes (subduction-related, intraplate, rifting), their similarities suggest the common origin of their geochemical features. Their characteristics are consistent with a HIMU-like mantle (high U/Pb). The $^{3}He/^{4}He$ ratio of the HIMU end-member is (6.8 ± 0.9 Ra, Hanyu and Kaneoka, 1997; Moreira and Kurz, 2001).

At Stromboli, He isotopic ratios in free gases and thermal waters match data from fluid inclusions in olivine and pyroxene. This shows that the isotopic signature is maintained as the gas ascends toward the surface, confirming that the maximum $^{3}He/^{4}He$ ratio of fluids generally reflects degassing of magmatic bodies at depth (Martelli et al., 2004).

On Panarea, highly degassed magma and small quantities of He in samples meant that neither abundances nor $^{3}He/^{4}He$ isotopic ratios could be measured. This was only possible in two pyroxene samples from Punta Torrione (“brown tuff” in the literature) and Punta del Tribunale (Castello formation; Calanchi et al., 2002).

The two samples from Panarea display very different $^{3}He/^{4}He$ ratios and He abundances. The Castello formation sample is very low in He and has a $^{3}He/^{4}He$ ratio of 3.39 Ra, whereas the Punta Torrione sample has a $^{3}He/^{4}He$ ratio of 5.1 Ra, like that measured at Salina and Vulcano (Martelli et al., 2008). The latter value may confirm that the source of

brown tuff is located beyond Panarea, within the La Fossa Caldera of Vulcano (Lucchi et al. 2010).

At Stromboli and Panarea, olivine and pyroxene have low $^{40}Ar/^{36}Ar$ ratios, in the range of subduction-related volcanism, well below typical mantle values (Burnard et al., 1997; Fischer et al., 2005) and close to the atmospheric signature ($^{40}Ar/^{36}Ar = 295.5$).

Lastly, this study aimed at measuring He and Ar isotopic ratios in quartz crystals, in particular in the quartz xenoliths of the Omo formation on Stromboli. Results show that the use of these crystals to determine abundances of He and consequently the $^{3}He/^{4}He$ isotopic ratios are unsatisfactory. Our data show diffuse, selective loss of He with respect to Ar in the quartz crystals, matching the data of Watson and Cherniak (2003) on diffusion of Ar in quartz, which is much lower than that of He.

The high Ar abundances measured, comparable to or more abundant than those of the olivine and pyroxene of all samples, probably indicates that the low values of Rc/Ra in the quartz xenoliths are due to loss of He by diffusion. This supports the hypothesis that fluids were released by a basaltic magma, partly trapped as fluid and melt inclusions, in accordance with the model in which partial melting of crustal rocks occurred in the middle-lower crust, forming rhyolitic melts + CO_2 fluids (Zanon et al., 2003).

References

Armienti, A., Francalanci, L., Landi, P., 2007. Textural effects of steady state behaviour of the Stromboli feeding system. J. Volcanol. Geoth. Res. 160, 86–98.

Argnani A, Savelli C (1999); "Cenozoic volcanism and tectonics in the southern Tyrrhenian Sea: space-time distribution and geodynamic significance". Geodynamics 27:409-432.

Barberi F., Gasparini P., Innocenti F., Villari L., (1973); "Volcanism of the southern Tyrrhenian Sea and its geodynamic implications". J. Geophys. Res., 78, 5221.

Barberi F., Innocenti F., Ferrara G., Keller J., Villari L., (1974); "Evolution of Eolian Arc volcanism (Southern Tyrrenian Sea)". Earth Pla, Sc. Lett., 21, 269-276.

Barberi F, Bizouard H, Capaldi G, Ferrara G, Gasparini P, Innocenti F, Joron JL, Lambert B, Treuil M, Allegre C (1978) Age and nature of basalts from the Tyrrhenian Abyssal Plain. In: Hsu K, Montadert L, et al. (eds) Init Rep Deep Sea Drilling Project. Washington, 42: pp 509-514

Beccaluva L., Di Girolamo P., Serri G. (1985); "High-K calc-alkaline, shoshonitic and leucititic volcanism of Campania (Roman Province, Southern Itlay): Trace element constraints on the genesis of an orogenic volcanism in a post-collisional extensional setting". In Science Assembly: Potassic Volcanism – Etna Volcano, edited by IAVCEI, Springer-Verlag, New York.

Beccaluva L., Brotzu P., Macciotta G., Morbidelli L., Serri G., Traversa G., (1989); "Cainozoic tectonomagmatic evolution and inferred mantle sources in the Sardo-Tyrrenian area." Acc. Naz. Lincei, The Lithosphere in Italy, 229-248.

Beccaluva L. et al., (1990); "Geochemistry and mineralogy of volcanic rocks from ODP sites 650, 651, 655 and 654 in the Tyrrhenian Sea" ; in Proceedings of the Ocean Drilling Program, Scientific Results, edited by N.J. Stewart, pp.49-73, U.S. Govt. Print. Off., Washington, D.C.

Beccaluva L, Coltorti M, Galassi B *et al* (1994) The Cainozoic calcalkaline magmatism of the western Mediterranean and its geodynamic significance. Boll Geofis Teor Appl 36:293-308

Bertagnini A, Metrich N, Landi P, Rosi M (2003); "Stromboli volcano (Aeolian Archipelago, Italy): an open window on the deep-feeding system of a steady state basaltic volcano". J Geophys Res 108, B7, 2336, doi:10.1029/2002JB002146.

Boyce, A.J., Fulignati, P., Sbrana, A., 2003. "Deep hydrothermal circulation in a granite intrusion beneath Larderello geothermalnarea (Italy): constraints from mineralogy, fluid inclusions and stable isotopes". J. Volcanol. Geotherm. Res. 126, 243–262

Burnard P., Graham D., Turner G., (1997); "Vesicle-specic noble gas analysis of `popping rock': Implications for primodial noble gases". Earth, Science 276 568-571

Calanchi N., Capaccioni B., Martini M., Tassi F., Valentini L., (1995); "Submarine gas-emission from Panarea Island (Aeolian Archipelago): distribution of inorganic and organic compounds and inferences about source conditions". Acta Vulcanologica, 7 (1), 43-48.

Calanchi N., Peccerillo A., Tranne C.A., Lucchini F., Rossi P.L., Kempton P., Barbieri M., Wu T.W., (2002); "Petrology and geochemistry of volcanic rocks from the island of Panarea: implications for mantle evolution beneath the Aeolian island arc (southern Tyrrenian Sea)". Journ. Volc. Geoth. Res., 115, 367-395.

Calanchi N., Tranne C.A., Lucchini F., Rossi P.L., Villa I.M., (1999); "Explanatory notes to the geological map (1: 10,000) of Panarea and Basiluzzo islands (Aeolian Arc. Italy)". Acta Vulcanologica, 11 (2), 223-243.

Capasso G.,· Carapezza M. L, Federico C., Inguaggiato S., Rizzo A. (2005); "Geochemical monitoring of the 2002–2003 eruption at Stromboli volcano (Italy): precursory changes in the carbon and helium isotopic composition of fumarole gases and thermal waters". Bull Volcanol 68: 118–134

Caliro, S., A. Caracausi, G. Chiodini, M. Ditta, F. Italiano, M. Longo, C. Minopoli, P. M. Nuccio, A. Paonita, and A. Rizzo (2004); "Evidence of a recent input of magmatic gases into the quiescent volcanic edifice of Panarea, Aeolian Islands, Italy, Geophys". Res. Lett., 31, L07619, doi:10.1029/2003GL019359.

Caracausi, A., R. Favara, S. Giammanco, F. Italiano, A. Paonita, G. Pecoraino, A. Rizzo, and P. M. Nuccio (2003); "Mount Etna:Geochemical signals of magma ascent and unusually extensive plumbing system", Geophys. Res. Lett., 30(2), 1057, doi:10.1029/2002GL015463.

Carapezza ML, Federico C (2000); "The contribution of fluid geochemistry to the volcano monitoring of Stromboli". J Volcanol Geotherm Res 95:227–245.

Carminati E, Wortel MJR, Spakman W, Sabadini R (1998); "The role of slab detachment processes in the opening of the western-central Mediterranean basins: some geological and geophysical evidence". Earth Planet Sci Lett 160:651-665.

Cella, F., Fedi, M., Florio, G. and Rapolla, A.: Gravity modelling of the litho-asthenosphere system in the Central Mediterranean, *Tectonophys*, 287, (1998), 117-138.

Chiarabba, C., De Gori, P., Speranza, F., (2008). "The southern Tyrrhenian suduction zone: deep geometry, magmatism and Plio-Pleistocene evolution". Earth and Planetary Science Letters 268, 408–423.

Crisci GM, De Rosa R, Esperança S, Mazzuoli R, Sonnino M (1991). "Temporal evolution of a three component system: the Island of Lipari (Aeolian Arc, southern Italy)". Bull Volcanol 53:207-221.

Dallai L., Magro G, Petrucci E, Ruggieri G. (2005). "Stable isotope and noble gas isotope compositions of inclusion fluids from Larderello geothermal field (Italy): Constraints to fluid origin and mixing processes". Journal of Volcanology and Geothermal Research 148 152– 164

De Astis G, Peccerillo A, Kempton PD, La Volpe L, Wu TW (2000). "Transition from calc-alkaline to potassium-rich magmatism in subduction environments: geochemical and Sr, Nd, Pb isotopic constraints from the island of Vulcano (Aeolian arc)". Contrib Mineral Petrol 139:684-703

De Astis G, Ventura G, Vilardo G (2003). "Geodynamic significance of the Aeolian volcanism (Southern Tyrrhenian Sea, Italy) in light of structural, seismological and geochemical data". Tectonics doi:10.1029/2003TC001506

De Astis, G., P. D. Kempton, A. Peccerillo, and T. W. Wu (2006). "Trace element and isotopic variations from Mt. Vulture to Campanian volcanoes: Constraints for slab detachment and mantle inflow beneath southern Italy". Contrib. Mineral. Petrol., 151, 331–351

De Gori P., Cimini G.B., Chiarabba C., De Natale G., Troise C., Deschamps A., (2001). "Teleseismic tomography of the Campanian volcanic area and surrounding Apenninic belt". J. Volcanol. Geoth. Res., 109, 55-75.

Della Vedova B, Bellani S, Pelli G, Squarci P (2001). "Deep temperatures and surface heath distribution. In: Vai GB, Martini PI (eds) Anatomy of an Orogen. The Apennines and the adjacent Mediterranean basins". Kluwer, Dordrecht, pp 65-76

Di Carlo I, Pichavant M, Rotolo SG, Scaillet B (2006). Experimental Crystallization of a High-K Arc Basalt: the Golden Pumice, Stromboli Volcano (Italy). Journal of Petrology, 47 (7), 1317-1343.

Di Liberto V. (2003). Mantle-crust interactions under the Aeolian arc: inferences from He and Sr isotopes . PhD thesys in Geochemistry.

Doglioni C., Gueguen E., Harabaglia P., Mongelli F., (1999); "On the origin of west-directed subduction zones and applications to the western Mediterranean". In Durand B., Jolivet L., Horvath F., Seranne M., (eds) The Mediterranean Basin: Tertiary Extension within the Alpine Orogen. Geological Society, London, Special Publications, 156, 541-561

Doglioni C, Innocenti F, Morellato C, Procaccianti D, Scrocca D (2004); "On the Tyrrhenian Sea opening". Mem Descr Carta Geol It 64:147-164

Dunai T.J., Baur H., (1995); "Helium, neon, and argon systematics of the European subcontinental mantle: Implications for its geochemical evolution". Geoch. Cosm. Acta, 59 (13), 2767-2783.

Ellam R.M., Hawkesworth C.J., Menzies M.A., Rogers M.W., (1989); " The volcanism of Southern Italy: role of subduction and the relationship between potassic and sodic alkaline magmatism". J. Geophys. Res., 94, 4589-4601.

Esperança S, Crisci GM, De Rosa R, Mazzuoli R (1992); "The role of the crust in the magmatic evolution of the Island of Lipari (Aeolian Islands, Italy)". Contrib Mineral Petrol 112:450-562.

Faggioni, O., Pinna, E., Savelli C. and Schreider, A.A.: Geomagnetism and age study of Tyrrhenian seamounts, *Geophys. J. Int.*, 123, (1995), 915-930.

Falsaperla S, Lanzafame G, Longo V, Spampinato S (1999); "Regional stress field in the area of Stromboli (Italy): insights into structural data and crustal tectonic earthquakes". J Volcanol Geotherm Res 88:147-166.

Farley K.A., Neroda E., (1998); "Noble gases in the Earth's mantle." Annu. Rev. Earth Planet. Sci., 26, 189-218.

Favali, P., Beranzoli L., Maramai A. (2004). Review of the tyrrhenian sea seismicity: how much is still to be unknown?, in from seafloor to deep mantle: architecture of the tyrrhenian back-arc basin, edited by. Marani MP, Gamberi F. and Monatti E, Mem. Descr.C. Geol. Ital., LXIV, 57-70.

Fechtig H. and Kalbitzer S. (1966); "The diffusion of argon in potassium bearing solids". In Potassium-Argon Dating (eds. O. A. Schaeffer and J. Zahringer), pp. 68–106. Springer.

Finetti I, Del Ben A (1986); Geophysical study of the Tyrrhenian opening". Boll Geofis Teor Appl 28:75-156 .

Finetti I., Morelli C., (1972); "Wide scale digital seismic exploration of the Mediterranean Sea. Boll. Geofis. Teor. Appl., 14, 291-342.

Finetti, J.R. : Innovative seismic highlights on the Mediterranean region. In *Geology of Italy*, Special Volume of the Italian Geological Society, (2004), 131-140.

Finizola A, Sortino F, L´enat JF Aubert M, Ripepe M, Valenza M (2003); "The summit hydrothermal system of Stromboli. New insights from self-potential, temperature, CO2 and fumarolic fluid measurements. Structural and monitoring implications".Bull Volcanol 65:486–504.

Finizola A, Sortino F (2003); "Preliminary model of fluid circulation at Stromboli volcano inferred by water and gas geochemistry". ICGG7-A-00108, 22-26 September 2003 Freiberg, Germany

Francalanci L., Manetti P., Peccerillo A., Keller J., (1993); "Magmatological evolution of the Stromboli volcano (Aeolian Arc, Italy): inferences from major and trace element and Sr isotopic composition of lavas and pyroclastic rocks". Acta Vulcanologica, 3, 127-151.

Francalanci L., Taylor S.R., McCulloch M.T., Woodhead J.D., (1993); " Geochemical and isotopic variations in the calc-alkaline rocks of Aeolian arc, southern Tyrrenian Sea, Italy: constraints on magma genesis". Contr. Min. Petrol., 113, 300-313.

Francalanci L, Tommasini S, Conticelli S, Davies GR (1999); "Sr isotope evidence for short magma residence time for the 20th century activity at Stromboli volcano, Italy". Earth Planet Sci Lett 167:61-69.

Francalanci L, Avanzinelli R, Petrone CM, Santo A (2004); "Petrochemical and magmatological characteristics of the Aeolian Arc volcanoes, southern Tyrrhenian Sea, Italy: inferences on shallow level processes and magma source variations". Per Mineral 73:75-104.

Francalanci L., Davies GR, Lustenmhower W. Tommasini S., Mason P., Conticelli S. (2005). Intra-grain Sr isotope evidence for crystal re-cycling and multiple magma reservoirs in the recent activity of Stromboli volcano, southern Italy, *J. Petrol.* 46 **(**10), pp. 1997–2005.

Gabbianelli G, Gillot PY, Lanzafame G, Romagnoli C, Rossi PL (1990); "Tectonic and volcanic evolution of Panarea (Aeolian Islands, Italy)". Mar Geol 92:313-326

Gabbianelli G., Romagnoli G., Rossi P.L., Calanchi N., (1993); "Marine geology of the Panarea-Stromboli area (Aeolian archipelago, Southeastern Tyrrhenian Sea)". Acta Vulcanologica, 3, 11-20.

Gasparini C., Iannaccone G., Scandone P., Scarpa R., (1982); "Seismotectonics of the Calabrian arc". Tectonophysics, 84, 267-286.

Gasperini D., Blichert-Toft J., Bosch D., Del Moro A., Macera P., Albarède F., (2002); "Upwelling of deep mantle material through a plate window: Evidence from the geochemistry of Italian basaltic volcanics". J. Geoph. Res., 107, NO.B12, 2367.

Gautheron C., Moreira M., (2002); "Helium signature of the subcontinental lithospheric mantle". Earth Plan. Sci. Lett., 199, 39-47.

Giardini D, Velona M (1991); "The deep seismicity of the Tyrrhenian sea". Terra Nova 3:57-64.

Gvirtzman Z, Nur A (1999); "The formation of Mount Etna as the consequence of slab rollback". Nature 401:782-785.

Gvirtzman Z., Nur A., (2001); "Residual topography, lithospheric structure and sunken slabs in the central Mediterranean". Earth Plan. Sci. Lett., 187, 117-130.

Harrison D., Barry T.L. and Turner G. (2004). Possible diffusive fractionation of helium isotopes in olivine and clinopyroxene phenocrysts, *European Journal of Mineralogy* 16, pp. 213–220

Hilton D.R., Hoogewerff J.A., Van Bergen M.J., Hammerschmidt K., (1992); "Mapping magma sources in the Sunda-Banda arcs, Indonesia: Constraints from helium isotopes". Geoch. Cosm. Acta, 56, 851-859.

Hilton, D. R., K. Hammerschmidt, S. Teufel, and H. Friedrichsen (1993a); "Helium isotope characteristics of Andean geothermal fluids and lavas". Earth Planet. Sci. Lett., 120, 265–282.

Hilton, D. R., K. Hammerschmidt, G. Loock, andH. Friedrichsen (1993b); "Helium and argon isotope systematics of the central Lau Basin and Valu Fa Ridge: Evidence of crust/mantle interactions in a back-arc basin". Geochim. Cosmochim. Acta, 57, 2819–2841.

D.R. Hilton DR., J. Barling J. and Wheller G.E.(1995). Effect of shallow-level contamination on the helium isotope systematics of ocean-island lavas. *Nature* 373, pp. 330–333

Hilton DR**,** Grönvold K**.,** Macpherson CG**,** Castillo P. (1999). Extreme $^{3}He/^{4}He$ ratios in northwest Iceland: constraining the common component in mantle plumes. Earth and Planetary Science Letters, 173,1-2, 53-60

Hilton D.R., Macpherson C.G., Elliott T.R., (2000); "Helium isotope ratios in mafic phenocrysts and geothermal fluids from La Palma, The Canary Islands (Spain): implications for HIMU mantle sources". Geoch. Cosmoch. Acta, 64, 2119-2132.

Hilton D.R., Fischer T.P., Marty B., (2002); "Noble gases and volatile recycling at subduction zones". Rev. Mineral, 320-370.

Hippolyte JC, Angelier J, Roure F (1994) A major geodynamic change revealed by Quaternary stress patterns in the Southern Apennines (Italy). Tectonophysics 230:199-210

Inguaggiato S, Rizzo A (2004); "Dissolved helium isotope ratios in ground-waters: a new technique based on gas-water reequilibration and its application to a volcanic area". Appl Geochem 19:665–673

Italiano F., Nuccio P.M., (1991); " Geochemical investigations of submarine volcanic exhalations to the east of Panarea, Aeolian Islands, Italy." Journal of Volcanology and Geothermal Research, 46, 125-141.

Kastens K, Mascle J (1990); "The geological evolution of the Tyrrhenian Sea: an introduction to the scientific results of the ODP LEG 107". In: Kastens KA, Mascle J, et al. (eds) Proc Ocean Drilling Program, Scientific Results, 107: pp 3-26

Landi P, Métrich MN, Bertagnini A, Rosi M. (2004);"Dynamics of magma mixing and degassing recorded in plagioclase at Stromboli" (Aeolian Archipelago, Italy). Contrib Mineral Petrol 147:213–227 DOI 10.1007/s00410-004-0555-5.

Landi, P., Francalanci, L., Pompilio, M., Rosi, M., Corsaro, R.A., Petrone, C.M., Nardini, I., Miraglia, L, (2006). The December 2002–July 2003 effusive event at Stromboli volcano, Italy: an insight into the shallow plumbing system by petrochemical studies. J. Volcanol. Geotherm. Res. 155, 263–284.

Landi, P., Métrich, N., Bertagnini, A., Rosi, M. (2008a). Recycling and "re-hydration" of degassed magma inducing transient dissolution/crystallization events at Stromboli (Italy). J. Volcanol. Geotherm. Res. 174, 325–336.

Landi, P., Francalanci, L., Corsaro, R.A., Petrone, C.M., Fornaciai, A., Carroll, M., Nardini, I., Miraglia, L. (2008b). Textural and Compositional Characteristics of the Lavas Erupted in the December 2002–July 2003 Effusive Events at Stromboli, Aeolian Island, Italy. In: "Learning fromStromboli and its 2002–2003 Eruptive Crisis", S. Calvari, M.Rosi,andM. Ripepe (edts), American Geophysical Union – Geophysical Monograph volume

Locardi E, Nicholich R (1988); "Geodinamica del Tirreno e dell'Appennino centro-meridionale: la nuova carta della Moho". Mem Soc Geol It 41:121-140

Lucchi F, Tranne CA, Rossi PL. (2010). Stratigraphic approach to geological mapping of the late Quaternary volcanic island ofLipari (Aeolian archipelago, southern Italy). 1-29, In Stratigraphy and geology of volcanic areas Di Gianluca Groppelli,Lothar Viereck-Goette

Marani MP, Trua T (2002);"Thermal constriction and slab tearing at the origin of a superinflated spreading ridge: Marsili volcano (Tyrrhenian Sea)". J Geophys Res 107, B2, 2188, doi:10.1029/2001JB000285.

Marani, M.P., (2004). "Super-inflation of a spreading ridge through vertical accretion". In: Marani, M.P., Gamberi, F., Bonatti, E. (Eds.), Memorie Descrittive della Carta Geologica d'Italia, vol. 64, pp. 185–194.

Martelli M. (2001); "Crust-mantle interaction along the Italian Peninsula: inferences from He isotope geochemistry in free gases and fluid inclusions". PhD thesis, Palermo University, pp. 84.

Martelli M, Nuccio PM, Stuart FM, Burgess R, Ellam RM, Italiano F (2004) "Helium-strontium isotope constraints on mantle evolution beneath the Roman Comagmatic Province, Italy". Earth Planet Sci Lett 224:295-308.

Martelli, M., P. M. Nuccio, F. M. Stuart, V. Di Liberto, and R. M. Ellam (2008); "Constraints on mantle source and interactions from He-Sr isotope variation in Italian Plio-Quaternary volcanism". Geochem. Geophys. Geosyst., 9, Q02001,doi:10.1029/2007GC001730

Martelli M., Renzulli A., Ridolfi F., Rizzo A., Rosciglione A.(2010). Definition of pre- and syn-eruptive volcanic processes – Task 1. Project DPC V2 – Paroxysm, Palermo – 18 Maggio 2010

Marty B., Trull T., Lussiez P., Basile I., Tanguy J.C., (1994); "He, Ar, O, Sr, and Nd isotope constraints on the origin and evolution of Mount Etna magmatism". Earth Plan. Sc. Lett., 126, 23-39.

Masarik J., Frank M., Schafer J. M., and Wieler R. (2001a); "Correction of in situ cosmogenic nuclide production rates for geomagnetic field intensity variations during the past 800,000 years". Geochim. Cosmochim. Acta 65 (*17*), 2995–3003.

Masarik J., Nishiizumi K., and Reedy R. C. (2001b); "Production rates of cosmogenic helium-3, neon-21 and neon-22 in ordinary chondrites and the lunar surface". Meteor. Planet. Sci. 36 (*5*), 643–650.

Matsumoto T., Chen Y., Matsuda J., (2001); "Concomitant occurrence of primordial and recycled noble gases in the Earth's mantle". Earth Pla. Sc. Lett., 185, 35-47.

Mongelli, F., Zito, G., De Lorenzo, S. and Doglioni C.: Geodynamic interpretation of the heat flow in the Tyrrhenian Sea, in *From Seafloor to Deep Mantle: Architecture of the Tyrrhenian Back-arc Basin*, edited by Marani M.P., Gamberi F. and Bonatti E., *Mem. Descr. Carta Geol. Ital.,* LXIV, (2004), 71-82.

Morelli C, Gantar C, Pisani M (1975); "Bathymetry, gravity and magnetism in the Strait of Sicily and in the Ionian Sea". Boll Geofis Teor Appl 65 39-58.

Morelli C, Pisani M, Gantar C (1975); "Geophysical anomalies and tectonics in the western Mediterranean". Boll Geofis Teor Appl 67:211-249.

Moore, J.N., Norman, D.I., Kennedy, B.M., (2001); "Fluid inclusion gas compositions from an active magmatic–hydrothermal system: a case study of the Geysers geothermal field, USA". Chem. Geol. 173, 3– 30

Naden, J., Kilias, S.P., Leng, M.J., Cheliotis, I., Sheperd, T.J., (2003). "Do fluid inclusions preserve y18O values of hydrothermal fluids in epithermal systems over geological time? Evidence from paleo- and modern geothermal systems, Milos island, Aegean Sea". Chem. Geol. 197, 143– 159.

Neri G., Caccamo D., Cocina O., Montalto A. (1996). Geodynamic implications of earthquake data in the southern Tyrrhenian sea. Tectonophysics, 258, 233-249.

Neri G, Barberi G, Orecchio B, Aloisi M, (2002); "Seismotomography of the crust in the transition zone between the southern Tyrrhenian and Sicilian tectonic domains". Geophys Res Lett 29:23 doi:10.1029/2002GL015562.

Niedermann S. (2002); "Cosmic-ray-produced noble gases in terrestrial rocks: Dating tools for surface processes". In Noble Gases in Geochemistry and Cosmochemistry, Vol. 47 (ed. D. Porcelli, C. J. Ballentine, and R. Wieler), pp. 731–777.

Nuccio PM, Valenza M (1998) "Magma degassing and geochemical detection of its ascent". Proc WRI-7 Balkema, Rotterdam, pp 475–478.

Nuccio P.M., Paonita A., Rizzo A, Rosciglione A. (2008). Elemental and isotope covariation of noble gases in mineral phases from Etnean volcanics erupted during 2001–2005, and genetic relation with peripheral gas discharges. Earth and Planetary Science Letters 272, 683–690

O'Nions R.K., Oxburgh E.R., (1988) ; "Helium volatile fluxes and the development of continental crust". Earth Plan. Sci. Lett., 90, 331-347.

Panza GF (1984) Structure of the lithosphere-asthenosphere system in the Mediterranean region. Ann Geophys 2:137-138

Panza GF (1984) The deep structure of the Mediterranean-Alpine region and shallow earthquakes. Mem Soc Geol It 29:5-13

Panza GF, Pontevivo A (2004) The Calabrian Arc: a detailed structural model of the lithosphere-asthenosphere system. Rend Accad Naz Sci dei XL, Mem Sci Fis Nat 28:51-88

Panza GF, Pontevivo A, Chimera G, Raykova R, Aoudia A (2003) The lithosphere-asthenosphere: Italy and surroundings. Episodes 26:169-174

Panza GF, Pontevivo A, Sarao' A, Aoudia A, Peccerillo A (2004); "Structure of the lithosphere-asthenosphere and volcanism in the Tyrrhenian Sea and surroundings". Mem Descr Carta Geol It 64:29-56

Parello F., Allard P., D'Alessandro W., Federico C., Jean-Baptiste P., Catani O., (2000); "Isotope geochemistry of Pantelleria volcanic fluids, Sicily Channel rift: a mantle volatile end-member for volcanism in southern Europe". Earth Plan. Sci. Lett., 180, 325-339.

Peccerillo A., (1985); "Roman Comagmatic Province (Central Italy) : evidence for subduction related magma genesis". Geology, 13, 103-106.

Peccerillo A., Kempton P.D, Harmon R.S., Wu T.W., Santo A.P., Boyce A.J., Tripodo A., (1993); "Petrological and geochemical characteristics of the Alicudi Volcano, Aeolian Islands, Italy: implications for magma genesis and evolution". Acta Vulcanologica, 3, 235-249.

Peccerillo A., Panza G.F., (1999); "Upper Mantle Domains beneath Central-Southern Italy: Petrological, Geochemical and Geophysical Constraints". Pure Appl. Geophys., 156, 421-443.

Peccerillo A., Wu T.W., (1992); "Evolution of Calc-alkaline Magmas in Continental Arc Volcanoes: Evidence from Alicudi, Aeolian Arc (Southern Tyrrenian Sea, Italy)". Journal of Petrology, 33, Part.6, 1295-1315.

Peccerillo A., (1999); "Multiple mantle metasomatism in central-southern Italy: Geohemical effects, timing and geodynamic implications". Geology, 27, 315-318.

Peccerillo A., (2001); "Geochemical similarities between Vesuvius, Phlegraean Fields and Stromboli volcanoes: petrogenetic, geodynamic and volcanological implications ". Miner. Petrol. 73, 93-105.

Pichler H., (1980); "The Island of Lipari". Rend. Soc. It. Min. Petr., 36 (1), 415-440.

Piromallo C., Morelli A. (1997); "Imaging the Mediterranean upper mantle by P-wave travel time thomography". Ann. Geofis. 40 (4), 963-979.

Piromallo C, Morelli A (2003); "P wave tomography of the mantle under the Alpine-Mediterranean area". J Geophys Res, 108, B2, 2065, doi: 10.1029/ 2002JB001757

Poreda R., Craig H., (1989); "Helium isotope ratios in circum-Pacific volcanic arcs". Nature, 338, 473-478.

Romano R, Villari L (1973) Caratteri petrologici e magmatologici del vulcanismo ibleo. Rend Soc It Mineral Petrol 29:453-484

Rosenbaum G., Lister GS. (2004). Neogene and quaternary rollback evolution of the tyrrhenian sea, the apennines, and the sicilian maghrebides. Tectonics, vol. 23, tc1013, pp 17. doi:10.1029/2003TC001518

Santo A.P., Chen Y., Clark A.H., Farrar E., Abebe Tsegaye, (1995); "$^{40}Ar/^{39}Ar$ ages of the Filicudi Island volcanics: implications for the volcanological history of the Aeolian arc, Italy". Acta Vulcanologica, 7 (1), 13-18.

Sapienza, G., D. R. Hilton, and V. Scribano (2005); "Helium isotopes in peridotite mineral phases from Hyblean Plateau (south-eastern Sicily, Italy)". Chem. Geol., 219, 115–129.

Savelli C (1988) Late Oligocene to Recent episodes of magmatism in and around the Tyrrhenian Sea: implications for the processes of opening in a young inter-arc basin of intra-orogenic (Mediterranean) type. Tectonophysics 146:163-181.

Savelli C, Gasparotto G (1994) Calc-alkaline magmatism and rifting of the deep-water volcano of Marsili (Aeolian back-arc, Tyrrhenian Sea). Mar Geol 119:137-157

Savelli C., (2002); "Time-space distribution of magmatic activity in the western Mediterranean and peripheral orogens during the past 30 Ma (a stimulus to geodynamic considerations)". Journal of Geodynamics, 34, 99-126.

Selli R, Lucchini F, Rossi PL, Savelli C, Del Monte M (1977); "Dati geologici, petrochimici e radiometrici sui vulcani centro-tirrenici". Giorn Geol 42:221-246

Selvaggi G. and Chiarabba C. (1995). Seismicity and P-wave velocity image of the Southern Tyrrhenian subduction zone. Geophysical Journal International, 121 (3), 818-826

Serri G (1990) Neogene-Quaternary magmatism of the Tyrrhenian region: characterization of the magma sources and geodynamic implications. Mem Geol Soc It 41:219-242.

Shuster D. L. and Farley K. A. (2004); "^{3}He/^{4}He thermochronometry". Earth Planet. Sci. Lett. 217 (*1–2*), 1–17.

Shuster D. L. and Farley K. A. (2004); "Diffusion kinetics of proton-induced 21Ne, 3He, and 4He in quartz". Geochimica et Cosmochimica Acta, Vol. 69, No. 9, pp. 2349–2359, 2005. Elsevier.

.Shuster D. L., Vasconcelos P. M., Heim J. A., and Farley K. A. (2005); "Weathering geochronology by (U-Th)/He dating of goethite". Geochim. Cosmochim. Acta 69 (*3*), 659–673.

Steinmetz, L., Ferrucci, F., Hirn, A., Morelli, C. and Nicolich, R.: A 550 km long Moho traverse in the Tyrrhenian Sea from O.B.S. recorded Pn waves, *Geophys. Res. Letts.*, 10, (1983), 428-431.

Stuart F.M., Ellam R.M., Harrop J.P., Fitton J.C., Bell B.R., (2000); "Constraints on mantle plumes from the Helium isotopic composition of basalt from the British Tertiary Igneous Province". Earth Pla. Sci. Lett., 117, 273-285.

Stuart F.M., Lass-Evans S., Fitton J.C. and Ellam R.M., (2003); "Extreme ^{3}He/^{4}He in picritic basalts from Baffin Islands: the role of a mixed reservoir in the mantle plumes". Nature, 424, 57-59.

Tonarini S, Armienti P, D'Orazio M, Innocenti F (2001); "Subduction-like fluids in the genesis of Mt. Etna magmas: evidence from boron isotopes and fluid mobile elements". Earth Planet Sci Lett 192:471-483.

Tonarini S., Leeman W.P., Ferrara G., (2001); "Boron isotopic variations in lavas of the Aeolian volcanic arc, South Italy." J. Volcanol. Geoth. Res., 110, 155-170.

Tranne C.A., Calanchi N., Gasparotto G., Rossi P.L., (1997); "Un esempio di applcazione delle unità stratigrafiche a limiti inconformi (UBSU): contributo alla nuova carta geologica dell'isola di Lipari (scala 1:10.000)". Convegno Ann. GNV, Poster session Rome.

Tranne CA, Lucchi F, Calanchi N, Rossi PL, Campanella T, Sardella A (2002); "Geological map of Filicudi (Aeolian Islands)". University of Bologna, LAC Florence.

Trua T., Clocchiatti R., Schiano P., Ottolini L., Marani M.; "The heterogeneous nature of the Southern Tyrrhenian mantle: Evidence from olivine-hosted melt inclusions from back-arc magmas of the Marsili seamount". Lithos 118 (2010) 1–16.

Trua, T., Serri, G., Marani, M., Renzulli, A., Gamberi, F., 2002. "Volcanological and petrological evolution of Marsili seamount (southern Tyrrhenian Sea)". Journal of Volcanology and Geothermal Research 114, 441–464.Trua, T., Serri, G., Marani, M., 2003. "Lateral flow of African mantle below the nearby Tyrrhenian plate: geochemical evidence". Terra Nova 15, 433–440.

Trua, T., Serri, G., Marani, M., 2007. "Geochemical features and geodynamic significante of the southern Tyrrhenian backarc basin". In: Beccaluva, L., Bianchini, G., Wilson, M. (Eds.), Geological Society of America, Special Paper, vol. 418, pp. 221–233.

Trull T. W., Kurz M. D., and Jenkins W. J. (1991); "Diffusion of cosmogenic 3He in olivine and quartz: Implications for surface exposure dating". Earth Planet. Sci. Lett. 103**,** 241–256.

Trull T. W. and Kurz M. D. (1993); "Experimental measurements of 3He and 4He mobility in olivine and clinopyroxene at magmatic temperatures". Geochim. Cosmochim. Acta 57**,** 1313–1324.

Vaggelli G., Belkin H.E., Francalanci L., (1993); "Silicate-melt inclusions in the mineral phases of the Stromboli volcanic rocks: a contributionto the understanding of magmatic processes". Acta Vulcanologica, 3, 115-125.

Vaggelli G, Francalanci L, Ruggieri G, Testi S (2003); "Persistent polybaric rests of calc-alkaline magmas at Stromboli volcano, Italy: pressure data from fluid inclusions in restitic quartzite nodules". Bull Volcanol 65:385-404.

Verzhbitskii, E.V. (2007) Heat Flow and Matter Composition of the Lithosphere of the World Ocean, *Oceanology*, 47, n.4, 564-570.

Vityk, M., Krouse, H.R., Demihov, Y., 1993; "Preservation of y18O values of fluid inclusion water in quartz over geological time in an epithermal environment: Beregovo Deposit, Transcarpathia, Ukraine. Earth" Planet. Sci. Lett. 119, 561– 568.

Watson E. B. and Cherniak D. J. (2003); "Lattice diffusion of Ar in quartz, with constraints on Ar solubility and evidence of nanopores". Geochim. Cosmochim. Acta 67 (*11*), 2043–2062.

Westaway R., (1992); "Seismic moment summation for historical earthquakes in Italy: Tectonic implications". J. Geophys. Res., 97, 15, 437-464.

Westaway R. (1993). Quaternary Uplift of Southern Italy. Journal of Geophysical Research, 98, no B12, pp. 21,741-21,772

Williams, A. J., F. M. Stuart, S. J. Day, and W. M. Phillips(2005); "Timing and rate of landscape development in central Gran Canaria, eastern Atlantic Ocean, from cosmogenic 3He concentrations in pyroxene microphenocrysts, Quat". Sci. Rev., 24, 211–222.

Zanon V, Frezzotti ML, Peccerillo A (2003); "Magmatic feeding system and crustal magma accumulation beneath Vulcano Island (Italy): evidence from fluid inclusions in quartz xenoliths". J Geophys Res, 108, B6, 2298, doi:10.1029/2002JB002140

Appendix A

Place	Sample	Location N	Location E	Water depth (m)	Stratigraphic unit	Rock type	Classification
Marsili	MRS 04	39°23'15"	14°27'53"	3050-2725		lavas	Island Arc Basalt lavas (IAB)
Panarea	Castello formation	38°38'01"	15°04'30"		Castello	lavas	HKCA andesite lava flows
Panarea	Punta Torrione	38°37'46.7"	15°04'16.1"		Punta Torrione	lavas	CA basaltic andesite/andesite
Stromboli	HP magma	38°47'34.8"	15°12'57.7"		La petrazza	scoria/ lavas	HK-basalts/basaltic shoshonites highly porphyritic
Stromboli	LP magma	38°47'34.8"	15°12'57.7"		Blond lavas	pumice	HK-basalts/basaltic shoshonites low porphyritic
Stromboli	SBX	38°48'23"	15°14'10"		San Bartolo lavas	Ultramafic Xenolithics	wehrlite
Stromboli	Quartz Xenoliths	38°47'33.7"	15°14'16"		Omo lavas	quartzite nodules	calc-alkaline basaltic andesite lavas
Stromboli	Omo lava	38°47'33.7"	15°14'16"		Omo lavas	lavas	calc-alkaline basaltic andesite lavas

Table I - *Sampling location and rock-type*

Appendix B

Sample	SiO2	TiO2	Al2O3	P2O5	Fe2O3	MgO	MnO	CaO	Na2O	K2O	LOI
	wt %	*wt %*	*wt %*	*wt %*	*wt %*	*wt %*	*wt %*	*wt %*	*wt %*	*wt %*	*wt %*
MRS 4	49.2	1.05	16.9	0.21	8.94	7.72	0.13	11.15	3.151	0.45	1.02
Castello Formation	61.17	0.55	15.98	0.17	6.95	3.36	0.11	6.63	2.55	2.53	0.9
Punta Torrione	60.03	0.72	17.41	0.09	7.00	2.72	0.14	6.91	2.95	2.05	0.09
HP magma	49.85	0.99	18.08	0.44	8.79	5.95	0.16	10.78	2.60	2.07	0.28
Lp magma	49.93	0.95	17.09	0.52	9.27	6.35	0.20	11.11	2.52	2.05	0.51
San Bartolo xenolithics	44.55	0.25	3.63	0.14	11.71	28.61	0.19	9.67	0.43	0.24	0.70
San Bartolo lavas	54.22	0.93	19.84	0.44	6.75	2.40	0.15	8.08	2.80	4.26	0.14
Omo lavas	55.65	0.81	17.83	0.21	7.70	3.95	0.20	8.52	2.86	2.01	0.26

Sample	Rb	Sr	Y	Nb	Zr	Cr	Ni	Ba	La	Ce	V	Co
	ppm	*ppm*	*ppm*	*ppm*	*ppm*	*ppm*	*ppm*	*ppm*	*ppm*	*ppm*	*ppm*	*ppm*
MRS 4	47	344	23	9	118	125	65	162	26	55	195	68
Castello Formation	80	479	24	7	107	35	10	418	22	40	193	19
Punta Torrione	8.4	157	5.9	0.4	14.7	9.4	7.6	98.4	11.9	22.3	125	8.7
HP magma	63	725	24	17	145	49	44	902	43	92	260	30
Lp magma	62	521	12	14	95	48	50	872	38	90	274	30
San Bartolo xenolithics	9.1	90	6.9	2	25	800	596	120	5	12	127	110
San Bartolo lavas	111	485	n.d	18	72	29	21	1407	38	93	198	n.d
Omo lavas	46	443	20	4	89	92	31	640	47	98	215	25

Table II- *Chemical analyses of samples rock*

Appendix C

Samples preparation for Fluid Inclusions study.

In order to get the necessary amount of phenocrysts for fluid inclusion analyses, lava and lapilli sampled were broken into small pieces by mechanical disintegration through a jaw crusher (Retsch BB200). After that the sample werw sieved using three different sievers of 2,1 and 0.5 mm. From the 0.5-1 mm fraction, olivine and clinopyroxene phenocrysts were separated at first through magnetic concentration (by Frantz isodynamic magnetic separator) and after several thousand of olivine and pyroxene for each sample were handpicked under a and fluid inclusion-bearing olivine were careful selected.

The crystals with small pieces of basalt adhering were eliminated together with those displaying alteration or iron tarnish. Aim of this operation was to make samoples as much as possible pure and free from alteration. In general sample weight in order of 2.0 to 4.0 g should be sufficient for two replicate analysis.

Fig. C.1 *– Jaw crusche (Retsch BB200) at INGV – Palermo.*

Fig. C.2 *– Shaker for sieves*

Fig. C.3 *– Franz magnetic separator (CFTA)*

This part of work had required much time and patience. Separates minerals, free of adhering matrix, were cleaned in an ultrasonic bath, with three cycles of 10 minutes, two in distelled water and one in acetone and then dried prior to loading into crushing device.

Crushing procedure

As result of the above discussion, crushing extraction were carried out on our mineral samples with the intent of chemically and isotopically analyzing the nobles gases trapped in fluid inclusion. The sample crusher used for this work had been devoloped in our group and was designed to hold a single stinless-steel sample containers into which about 1-2 g of olivine or pyroxene grains can be loaded (fig 2).

The amount of sample material used foe each analyses is function of the expected amount of gas trapped and of the pressure of trapping.

Fig. C.4 *– Binocular microscope for manual picking.*

The crushing device consists of a piston/cylinder operated by a hydraulic press and crusher chamber where the inclusion gases are released. A pressure control system permits to gradually increase the acting pressure on the grain samples. After sample loading, the sample chamber and all extraction lines (under pumping) are heated to ≈125°C overnight, in order to reduce gas adsorption and to induce immediate release of the adsorbed volatiles into the detection system. At the beginning of each day, before the sample run, an eventual presence of gas leaks was checked by perfming a procedural blank (crusher blank hereafter) by operating the detection system prior to crushing. Typical crusher blank levels (in term of partial pressures) were 1×10^{-14} and 1×10^{-11} mbar for ^{4}He and ^{36}Ar, respectively.

Short crush times werw employed to help avoid the release of extraneous volatiles contained in crystal lattice sites.

For calibrating the real fluid inclusion release by crusching olivine, some analyses were run by simulating crush action with an empty sample chamber, and crushing inclusion-free pieces of synthetic degassed quartz.

Gas liberated by sample crushing are then expanded into the 976 cm^3 gas preparation line. The gas preparation section serves to remove reactive gases and partition the noble gases into two fraction, He + Ne and Ar.

Helium and Neon were isolated from other components by sequential exposure to (i) two Ti getters at 250 °C. (ii) two liquid nitrogen-cooled charcoal traps, and (iii) a liquid He-cooled charcoal traps (14°K). Then, Helium is separated from Neon at 35° K and Neon is successively released heating at 75 °K the cryostat. These gases were introduced successively into the VG 5400 mass spectrometer. Argon is concentrated in the charcooal traps and subsequently released by heating that, after He and Ne analyses. Mesassurements are made in static vacuum prior to residual sample evacuation using a dedicated ion pump.

Fig. C.5 *– Crusher devise installed at the noble gas lab of the INGV Palermo.*

The mass spectrometer sensitivity and the mass discrimination corrections for the noble gases were calibrated after each crushing run by analysis of gas aliquots of known volume and isotopic composition from gas pipettes.

After each analysis, the crusher was opened, the remnant of the crushing sieved using three sieves (0.5, 0.25 and 0.10 mm) and the four resulting fractions weighted for estimate the real amount of crushed sample.

The crushing procedure applied to the sample was rather successful, as the totality of the 20 analysed sample released an enough quantity of gas to be distinguished from blank and to be measured with very low analytical errors (see Tab 4).

The high performance of the VG 5400 helium spectrometer and the rigorous calibration procedure allow us to obtain very modest analytical errors. Several repeatability tests have displayed that the overall uncertainties of our isotopic data are below 1%.

Table X summarizes the results of helium, neon and argon analyses for gases extracted by vacuum crushing techniques.

Duplicate or triplicate analyses of the samples were carried out when sufficient quantities of olivine or pyroxene were available.

The nobles gases were analyzed in two magnetic sector noble gas mass spectrometer. The abundances of He, Ne and Ar isotopes were determined.

Acknowledgements

I wish to thank Prof. Nuccio and Dr. Italiano for scientific and human contributions.
An particularly acknowledgement to Prof. Stefano Bellia.
This thesis would not have been possible without the substantial support and facilities from Dip. CFTA and the members of its technical staff.
I'm also grateful to all the peaple working at the Istituto di Geofisica e Vulcanlogia (INGV) sez. Palermo, a special acknowledgement is due to Dr. M. Martelli for his inexhaustible assistance during part of the experimental period.
Many sincere thanks are due to friends of Dipartimento CFTA for their encouragement and assistance during these years .